UNIVERSIDADE FEDERAL DE SANTA CATARINA
CENTRO DE CIÊNCIAS FÍSICAS E MATEMÁTICAS
PROGRAMA DE PÓS-GRADUAÇÃO EM FÍSICA

Elisa Iahn Goettems

Quantum Correlations in DQC1 Model with Post-selection

Florianópolis
2020

Elisa Iahn Goettems

Quantum Correlations in DQC1 Model with Post-selection

Dissertação submetida ao Programa de Pós-Graduação em Física da Universidade Federal de Santa Catarina para a obtenção do título de mestre em Física.
Supervisor: Prof. Dr. Eduardo Inacio Duzzioni

Florianópolis
2020

Ficha de identificação da obra elaborada pelo autor,
através do Programa de Geração Automática da Biblioteca Universitária da UFSC.

Goettems, Elisa Iahn
Quantum Correlations in DQC1 Model with Post-selection / Elisa Iahn Goettems ; orientador, Eduardo Inacio Duzzioni, 2020.
72 p.

Dissertação (mestrado) - Universidade Federal de Santa Catarina, Centro de Ciências Físicas e Matemáticas, Programa de Pós-Graduação em Física, Florianópolis, 2020.

Inclui referências.

1. Física. 2. Correlações quânticas. 3. DQC1. 4. Pós seleção. I. Duzzioni, Eduardo Inacio. II. Universidade Federal de Santa Catarina. Programa de Pós-Graduação em Física. III. Título.

Elisa Iahn Goettems

Quantum Correlations in DQC1 Model with Post-selection

O presente trabalho em nível de mestrado foi avaliado e aprovado por banca examinadora composta pelos seguintes membros:

Prof. Dr. Diogo de Oliveira Soares Pinto
IF-São Carlos USP

Prof. Dr. Marcelo Henrique Romano Tragtenberg
UFSC

Certificamos que esta é a **versão original e final** do trabalho de conclusão que foi julgado adequado para obtenção do título de mestre em Física.

Documento assinado digitalmente
Ivan Helmuth Bechtold
Data: 30/03/2020 15:09:46-0300
CPF: 895.230.409-87

Coordenação do Programa de
Pós-Graduação em Física

Documento assinado digitalmente
Eduardo Inacio Duzzioni
Data: 30/03/2020 16:17:23-0300
CPF: 003.513.789-44

Prof. Dr. Eduardo Inacio Duzzioni
Orientador

Florianópolis, 2020.

This work is dedicated to all those who supported and believed in me.

ACKNOWLEDGEMENTS

I would first like to thank my advisor Prof. Dr. Eduardo Duzzioni and my almost co-advisor Dr. Thiago Maciel for all the support and meetings that helped me to expand my knowledge on this interesting area.

In the same way, I would like to thank Prof. Dr. Diogo Soares Pinto for the most profitable fifteen days and full of fruitful conversations about my work. As Ana Sprotte for helping me at the beginning of this research. I would like to especially thank Susane for all the help and discussions about MATLAB codes, as well as my classmates such as Antônio and Caio.

I thank my friends and colleagues who provided me with moments of relaxation that were essential for my mental health.

I thank UFSC and all its teachers, servers and technicians, especially the server Antonio Marcos Machado. And the research group GIQSul that provided afternoon full of knowledge.

I thank CNPQ and CAPES for financial support through scholarship and event assistance. Finally, I want to express all my affection towards my family, especially my boyfriend Rafael Brito for all help and support, even without understanding much of my work, during the years of research and writing of the dissertation, my gratitude and love can not be expressed in words. Thank you.

“If knowledge can create problems, it is not through ignorance that we can solve them.”
(Isaac Asimov, 1972)

RESUMO

Neste trabalho estudou-se as correlações quânticas de emaranhamento, não-localidade de Bell, discórdia quântica e coerência, no modelo de Computação Quântica Determinística com um Qubit (DQC1). Como sugerido em algumas literaturas, o emaranhamento não é o recurso quântico responsável pela vantagem sobre a Computação Clássica para calcular o traço normalizado de qualquer matriz unitária. Para o caso estudado, DQC1 com dois qubits (qubit de controle e um auxiliar), encontramos emaranhamento nulo, como esperado de estudos anteriores na literatura. Portanto, adicionamos uma pós-seleção com um filtro específico ao final do circuito a fim de promover outras correlações quânticas como emaranhamento e violação da desigualdade de Bell. Isso nos permitiu realizar um processo de purificação no qubit auxiliar através de um programa de otimização do parâmetro do filtro η e pureza do qubit auxiliar. Fizemos duas análises das correlações quânticas médias geradas: uma fixando o parâmetro do filtro cumulativo e executando 400 vezes o circuito DQC1 com a pós-seleção; e a outra com a otimização da pureza para que esta atingisse 0.99. Foi possível verificar o mesmo padrão nos gráficos da média dos valores das correlações quânticas para o DQC1 com 10^4 matrizes unitárias aleatórias e qubit de controle aleatório. Conseguimos alcançar violação da desigualdade de Bell e emaranhamento para uma pureza do qubit auxiliar pouco acima de 0.53. Analisamos a densidade de estados gerados pelas correlações quânticas e constatamos que conforme o parâmetro do filtro η aumenta acessamos menos estados com outras correlações quânticas como emaranhamento e violação da desigualdade de Bell. E verificamos, como esperado, que podemos ter violação da desigualdade de Bell apenas para estados emaranhados.

RESUMO EXPANDIDO

Introdução

A Mecânica Quântica surge no século XX em resposta a teorias de escala não atômica e busca explicar fenômenos antes sem uma teoria sólida. Essa teoria de caráter probabilístico surgiu em conjunto com a Teoria da Informação e Computação Quântica e apresentam fortes conexões principalmente no ramo da Mecânica Estatística com a formulação da Entropia. Outra característica em comum é a presença do conceito de correlação. Em informação quântica esta propriedade pode ser expressa em termos de uma quantidade chamada informação mútua, que detecta a quantidade de informação que pode ser obtida de uma variável aleatória ao analisarmos outra variável.

Em informação quântica a caracterização das correlações foi introduzida a partir de 1935 com o artigo de Einstein, Podolsky e Rosen (EINSTEIN; PODOLSKY; ROSEN, 1935) que propõem um experimento mental a fim de testar a completude da mecânica quântica. Em resposta ao paradoxo EPR, como ficou conhecido, Schrödinger (SCHRÖDINGER, 1935) estabeleceu o conceito de emaranhamento, que pode demonstrar uma característica não local da mecânica quântica. Se dois estados estão emaranhados, uma medida em uma parte do sistema pode interferir na outra mesmo que estes estejam separadas espacialmente.

Foi em 1964 que John Bell (BELL, 1964) inventou uma maneira de testar se existem modelos de variáveis ocultas locais que completariam a mecânica quântica. Desenvolveu uma teoria que foi quantificada através de um conjunto de condições, atualmente conhecidas como desigualdades de Bell, que são violadas apenas para sistemas emaranhados. Aspect (ASPECT; GRANGIER; ROGER, 1982) foi o primeiro a verificar experimentalmente essas desigualdades e indicar aspectos não locais da mecânica quântica.

Foi somente a partir de 1980 que o emaranhamento passou a ser considerado um recurso disponível na natureza. Estados emaranhados foram usados para executar com eficiência tarefas que usavam anteriormente apenas recursos clássicos. O emaranhamento foi considerado a única manifestação de correlações quânticas em sistemas compostos até o final do século XX. Ollivier & Zurek (OLLIVIER; ZUREK, 2001) e Vidal & Werner (VIDAL; WERNER, 2002) mostraram que as correlações quânticas existem mesmo quando os sistemas são separáveis (sistemas sem emaranhamento). Essa classe de correlação foi chamada de discórdia quântica.

A correlação quântica chamada coerência só foi estudada em 2014 por Braumgratz et.al. (BAUMGRATZ; CRAMER; PLENIO, 2014) e descreve o caráter da superposição de estados em relação a uma determinada base de medida. A capacidade dos sistemas quânticos existirem em "estados de superposição" denota a incapacidade da física clássica em explicar certos conceitos, sendo o emaranhamento um deles. Diz-se que os estados em superposição possuem coerência quântica.

A computação quântica se desenvolveu bastante na última década. Com Feynman (FEYNMAN, 1982), observou-se que nenhum sistema clássico poderia simular com eficiência um sistema quântico. Existem alguns modelos computacionais universais diferentes para executar a computação quântica, entre eles: Circuital - onde um conjunto de qubits é inicializado em estados puros e uma sequência de operações lógicas é executada e ao final os qubits são medidos; Computação Adiabática - no qual é estabelecida uma evolução contínua do estado do sistema, os qubits de entrada são descritos pelo estado fundamental de um hamiltoniano inicial e o resultado da computação é expressa pelo estado fundamental do hamiltoniano final (FARHI et al., 2000); Computação baseada em medidas - com operações representadas por medidas e operações controladas (RAUSSENDORF; BROWNE; BRIEGEL, 2003), além de modelos restritos tal como a Computação Quântica Determinística com um Qubit (DQC1) - em que um conjunto de n qubits inicializado no estado maximamente misto e um qubit semi-puro, realizam o cálculo do traço normalizado de uma matriz unitária através da aplicação de uma porta unitária controlada pelo qubit semi-puro (KNILL; LAFLAMME, 1998).

Objetivos

Nesta dissertação discutiremos o modelo de Computação Quântica Determinística com um Qubit, que calcula o traço normalizado de qualquer matriz unitária de maneira mais eficiente que com a computação clássica (DATTA; SHAJI; CAVES, 2008). O objetivo é promover correlações quânticas, como emaranhamento e não-localidade de Bell, para esse modelo de computação restrito através de um processo de pós-seleção com a aplicação de uma porta filtro ao final do circuito.

Metodologia

Usamos o modelo de computação chamado DQC1 com a restrição de $n = 1$ qubit auxiliar, portanto, dois qubits, um auxiliar e um de controle. Temos formas fechadas para quantificadores de correlações com dois qubits. Usando uma rotina do MATLAB, geramos aleatoriamente 10^6 matrizes unitárias e estados iniciais do qubit de controle para calcular os valores de coerência, discórdia, emaranhamento e não-localidade de Bell, sendo encontrado valor nulo de emaranhamento e a não violação da desigualdade de Bell, como já explorado na literatura para este modelo. Com o objetivo de promover as outras correlações não alcançadas pelo modelo com dois qubits, foi usado o processo de pós-seleção com a aplicação de uma porta filtro com parâmetro η após o circuito DQC1 com dois qubits. Duas abordagens foram feitas neste ponto, uma fixando 13 valores cumulativos possíveis deste parâmetro, plotando a média dos valores atingidos pelas correlações geradas por 10^4 matrizes unitárias aleatórias (do filtro e da porta controlada uniária) e executando o processo de otimização 400 vezes. Também foram analisados os máximos da média de cada correlação para os diferentes η cumulativos. A outra abordagem foi um processo de otimização para alta pureza do qubit auxiliar,

plotando o mesmo que da primeira abordagem.

Resultados e Discussões

Detectamos que mesmo antes da pós-seleção tínhamos a coerência e discórdia quântica, sendo a primeira com valor máximo de 1 devido apenas ao qubit de controle e a segunda com valor não nulo. Obtivemos valores não nulos de emaranhamento e violação da desigualdade de Bell para as duas abordagens com pós-seleção. Notamos que conforme o parâmetro do filtro vai crescendo o valor das correlações diminui até recuperarmos os resultados com o modelo DQC1 sem a pós-seleção, ou seja fazendo $\eta = 1$ $(0 \leq \eta \leq 1)$ é o mesmo que não aplicarmos nenhum filtro no circuito DQC1. Notamos também que existe uma purificação mínima para que comece a ter emaranhamento e consequentemente violação da desigualdade de Bell. Analisamos ainda o progresso da densidade de estados para cada correlação com relação à probabilidade de sucesso. Temos muitos estados que apresentam coerência e discórdia quântica mas que não possuam emaranhamento e nem atingem a violação da desigualdade de Bell. Reparamos que conforme η aumenta, temos menos estados acessíveis com outras correlações quânticas (emaranhamento e violação da desigualdade de Bell).

Considerações finais

Com a análise dos gráficos obtidos para o máximo das correlações para os diferentes parâmetros do filtro, notamos que precisamos de uma pureza pouco acima de 0.5 para que tenhamos emaranhamento e aspectos não-locais. Assim, o processo de adicionar uma pós-seleção ao circuito DQC1 com dois qubits se mostrou eficiente quanto ao nosso objetivo de promover correlações quânticas antes não alcançadas. Podemos expandir ainda nossos estudos, executando o programa para uma quantidade maior de matrizes unitárias aleatórias e para um número maior de qubits auxiliares com o propósito de verificar se este comportamento se mantém, afim de implementar este processo de pós-seleção em algoritmos quânticos, como a Fatoração de Shor.

Palavras-chave: Computação Quântica. Correlações Quânticas. Modelo DQC1. Emaranhamento. Não localidade de Bell. Coerência. Discórdia Quântica.

ABSTRACT

In this work we studied the quantum correlations of entanglement, nonlocality of Bell, quantum discord, and coherence in the Deterministic Quantum Computation with One Qubit (DQC1) model. As suggested by some authors in literature, entanglement is not the quantum resource responsible for the advantage over Classical Computation to the calculation of the normalized trace of any unitary matrix. For the studied case, the DQC1 with two qubits (auxiliary and control), we find null entanglement, as expected from previous studies in literature. Therefore, a post-selection with a specific filter was added to the end of the circuit to promote other quantum correlations, such as entanglement and nonlocality of Bell. This allowed us realizing a purification process in the auxiliary qubit through an optimization program for the filter parameter η and the purity of the auxiliary qubit. We performed two analysis of the generated average quantum correlations: one sets the cumulative filter parameter and runs the DQC1 circuit 400 times with post-selection; and the other one with the optimization of the filter parameter so that the purity of the auxiliary qubit reaches 0.99. It was possible to verify the same pattern in the plots of the mean values of the quantum correlations for DQC1 with 10^4 random unitary matrices and random control qubit. We managed to achieve non null entanglement and the violation of Bell's inequality for the purity of the auxiliary qubit just over 0.53. We analyzed the density of states generated for these quantum correlations and found that as the filter parameter (η) increase we can access less states with others quantum correlations as entanglement, and violation of Bell's inequality. Also, as expected, we can have Bell's inequality violation only for entangled states.

Keywords: Quantum Computation. Quantum Correlations. DQC1 model. Entanglement. Bell's Nonlocality. Coherence. Quantum Discord.

LIST OF FIGURES

LIST OF TABLES

CONTENTS

1 INTRODUCTION

Quantum Mechanics (QM) emerges in the twentieth century in response to non-atomic scale theories such as Newton's laws of motion and to trying to explain previously unsupported phenomena such as the blackbody radiation and photoelectric effect. In conjunction with QM also emerged the theory of Quantum Information (QI), important for the improvement of communication devices. These two theories have very strong connections, especially in the field of Statistical Mechanics with the formulation of entropy. Another common feature is the presence of the concept of correlations. In QI this property can be expressed in terms of an amount called mutual information, which detects the amount of information that can be obtained from a random variable when analyzing another random variable.

In QM the characterization of correlations was introduced by Einstein, Podolsky, and Rosen (EINSTEIN; PODOLSKY; ROSEN, 1935) in a mental experiment in order to test the completeness of QM. The hypothesis of EPR (as it became known) assesses the philosophical nature of QM, whether it would fully describe the reality of a system, i.e., if the act of measuring alters or not the physical quantities being analyzed.

In response to the EPR paradox, Schrödinger (SCHRÖDINGER, 1935) established the concept of entanglement, which can demonstrate a non-local feature of QM. If a measurement is made on one part of the system it can alter the quantum state of the other part, even though they are spatially separated.

John Bell (BELL, 1964) developed a theory that satisfies the EPR criteria for completeness of QM by introducing additional variables (local hidden variables) and quantified it through a set of conditions, currently known as Bell's inequalities, that is violated only for entangled systems. Aspect (ASPECT; GRANGIER; ROGER, 1982) was the first to experimentally verify these inequalities indicating non-local aspects of QM.

Only then from 1980 entanglement is regarded as a resource available in nature and it was only with Werner in 1989 (WERNER, 1989) that nonlocality and entanglement became distinguishable correlations. Entanglement was defined as the correlation that can not be obtained with local operations and classical communication. Entangled states were used to efficiently perform tasks that previously used only classical resources. Entanglement was regarded as the only manifestation of quantum correlations (QC) in composite systems until the end of the twentieth century (HORODECKI; HORODECKI; HORODECKI; HORODECKI, 2009). However, Henderson & Vedral (HENDERSON; VEDRAL, 2001) and Ollivier & Zurek (OLLIVIER; ZUREK, 2001) have shown that QC exist even when systems are separable (non-entangled systems), this class of correlation has been called quantum discord. This correlation shows the signature of nonclassicality in quantum systems (DAKIĆ; VEDRAL; BRUKNER, 2010), (MODI; BRODUTCH, et al., 2012).

Coherence has only been refined in 2014 by Braumgratz et al. (BAUMGRATZ; CRAMER; PLENIO, 2014). This correlation describes the superposition character of states in relation to a given measurement basis. It is said that states in superposition possess quantum coherence. The capability of quantum systems to exist in "superposition states" denotes the incompleteness of Classical Physics to explain certain concepts related to massive objects.

Quantum computing has also been developed greatly in the last decade. There are tasks, as factoring integer numbers, that are solved efficiently with quantum computers (SHOR, 1994). It is believed that such speed up comes from the quantum correlations, as entanglement. However, this resource is not fully understood, and it has not yet been shown which resource is responsible for this advantage over classical computing. With Feynman (FEYNMAN, 1982) it was observed that no classical system could efficiently simulate a quantum system, then he proposed that only one quantum system would be able to simulate another of the same type. Subsequently, Deutsch (DEUTSCH, D., 1985) creates a Universal Quantum Computation Model that implements an efficient quantum algorithm (Deutsch's two qubits problem) better than any classical algorithm, also creating the quantum circuit language, very similar to the classical one (DEUTSCH, D. E., 1989). We have some different computational models to perform quantum computing that present solutions for some problems better than classical algorithms and do not require much resources, among them are:

- Circuital — a set of qubits is initialized in a pure state and a sequence of logical operations is performed. Bernstein-Vazirani algorithm (BERNSTEIN; BERNSTEIN, 1993), Shor algorithm (SHOR, 1994), and Simon algorithm (SIMON, D. R., 1997) are some examples of this model;

- Adiabatic Computation — a continuous evolution of the system state is made, the input qubits are described by the ground state of an initial hamiltonian and the computing solution is expressed by the ground state of the final hamiltonian (FARHI et al., 2000), (VAN DAM; MOSCA; VAZIRANI, 2001);

- Measurement-Based Computing — operations are represented by measures on the qubit in the entangled state (RAUSSENDORF; BROWNE; BRIEGEL, 2003), (BRIEGEL et al., 2009).

And we also have computational restricted model as

- Deterministic Quantum Computation with One Qubit (DQC1) — a set of n qubits is initialized in the maximally mixed state and a semi-pure qubit. The computation is performed by applying a unitary gate controlled by the semi-pure qubit (KNILL; LAFLAMME, 1998).

To have a speed up in relation to classical algorithms, quantum computing with pure states requires entanglement (JOZSA; LINDEN, 2003). However, as we know, this last restricted model (DQC1) requires little or no entanglement to performs a task (DATTA; FLAMMIA; CAVES, 2005). In this dissertation we will discuss in more details this model, which efficiently calculates the normalized trace of any unitary matrix (DATTA, 2008). Laynon et al. suggest that discord could be a necessary resource responsible for the quantum computational speed up in this model (LANYON et al., 2008). On the other hand, the responsible resource for this advantage over classical computation was not yet found. The goal of this work is to promote QC, for this restricted computing model, as entanglement and non-locality, that could not be achieved without a post-selection process.

The dissertation is divided as follows. In chapter two we approach the fundamental concepts for the basic understanding of the quantum processes, exposing among them the concept of density matrix and quantum circuits.

Quantum correlations may be responsible for the advantage of quantum computing over classical computing for this model. For this reason, in the third chapter we approach some measures of quantum correlations, as coherence, quantum discord, entanglement, and Bell's nonlocality, and the quantifiers that are used for the DQC1 model.

In the fourth chapter it is explained the quantum computation model DQC1, after that it is fixed in $n = 1$ the number of auxiliary qubits to study the QC that can be generated. The study of the promotion of certain quantum correlations not previously present in this model is still developed using the post-selection with a specific filter at the end of the circuit. Also, we analyse the density of states that have been generated randomly for each type of quantum correlation.

In the last chapter of this dissertation we overview of what can be expected from this promotion of correlations, what kind of QC can be achieved in more states after the post-selection, as well as the conclusion and perspectives.

2 FUNDAMENTAL CONCEPTS

The Quantum Mechanics provides the mathematical structure to develop the physical theories through a set a postulates (NIELSEN; CHUANG, 2000). We represent the fundamental element of Quantum Computation by a *qubit* or *quantum bit*. It is the quantum analogous of the classical bit. The qubit is represented by a two-dimensional basis (formed for two states). A Quantum Computer is based on the principles of Quantum Physics and maybe it is able to solve problems that Classical Computers yet can not solve.

Here we explore some basic concepts of QM and quantum circuits that are essential for understanding the DQC1 model. The content of this chapter is based on the references (NIELSEN; CHUANG, 2000; BALLENTINE, 2014; DE WOLF, 2019).

2.1 SUPERPOSITION PRINCIPLE

The mathematical description of a physical system is made by the linear algebra. The superposition is a fundamental principle of QM, which states that if we have two states of a quantum system, then any superposition should also be an allowed state of a quantum system, i.e, if a state can be in one of many system configurations, then, the general state can be written as a linear superposition of those states with complex coefficients. The idea of this principle is that all states are possible at the same time until the measurement is performed, that collapses the state and destroys the initial configuration.

2.2 THE QUANTUM BIT

A fundamental concept in Classical Information is the bit. It can assume two values: 0 or 1. We have an analog concept in Quantum Computation and QI, the qubit with two possible states $|0\rangle$ and $|1\rangle$. The *Dirac Notation* with '$|\,\rangle$' (ket) and '$\langle\,|$' (bra) summarized in Table 1 is the standard notation of the QM and will be amply used in this work. As described in the previous subsection, it is possible to form linear combinations of states as

$$|\psi\rangle = a|0\rangle + b|1\rangle\,,$$

where the states $|0\rangle$ and $|1\rangle$ are known as computational basis states, that form the orthonormal basis (two-dimensional Hilbert space), a and b are complex numbers normalized by

$$|a|^2 + |b|^2 = 1.$$

After the measurement, have the probability $|a|^2$ of the system being found in state $|0\rangle$ and the probability $|b|^2$ of being found in state $|1\rangle$. The computational basis can be

writing as

$$|0\rangle = \begin{bmatrix} 1 & 0 \end{bmatrix}^T, \quad |1\rangle = \begin{bmatrix} 0 & 1 \end{bmatrix}^T,$$

such that these states $|0\rangle$ and $|1\rangle$ also are eigenstates of the Pauli operator σ_Z with eigenvalues ± 1, respectively. We define the *Pauli Operators* represented in the computational basis as

$$\sigma_X = X = \begin{bmatrix} 0 & 1 \\ 1 & 0 \end{bmatrix}, \sigma_Y = Y = \begin{bmatrix} 0 & -i \\ i & 0 \end{bmatrix}, \sigma_Z = Z = \begin{bmatrix} 1 & 0 \\ 0 & -1 \end{bmatrix}. \tag{1}$$

These operators obey the following commutation and anti-commutation relations

$$[\sigma_i, \sigma_j] = 2i \sum_{k=1}^{3} \epsilon_{ijk} \sigma_k,$$
$$\{\sigma_i, \sigma_j\} = 2\delta_{ij} I,$$

where ϵ_{ijk} is the *Levi-Civita* symbol, δ_{ij} is the *Kronecker delta*, and I is the identity matrix.

We follow the geometric interpretation for a qubit in $\mathbb{R}^3$, which one can be rewritten as

Notation	Description
z^*	Complex conjugate of the number z
$\|\psi\rangle$	Vector state. Also known as *ket*
$\langle\psi\|$	Vector dual to $\|\psi\rangle$. Also known as *bra*
$\langle\varphi\|\psi\rangle$	Inner product between the vectors $\|\varphi\rangle$ and $\|\psi\rangle$
$\|\varphi\rangle \otimes \|\psi\rangle$	Tensor product of $\|\varphi\rangle$ and $\|\psi\rangle$
$\|\varphi\rangle\|\psi\rangle$	Abbreviated notation for tensor product of $\|\varphi\rangle$ and $\|\psi\rangle$
A*	Complex conjugate of the matrix A
A^T	Transpose of the matrix A
$A^\dagger$	Hermitian conjugate or adjoint of the matrix A, $A^\dagger = (A^T)^*$
$\langle\varphi\|A\|\psi\rangle$	Inner product between $\|\varphi\rangle$ and $A\|\psi\rangle$. Equivalently, inner product between $A^\dagger\|\varphi\rangle$ and $\|\psi\rangle$

Table 1 – Dirac Notation used in Quantum Mechanics.

$$|\psi\rangle = \cos\frac{\theta}{2}|0\rangle + e^{i\phi}\sin\frac{\theta}{2}|1\rangle,$$

with θ, $\phi \in \mathbb{R}$. The states $|0\rangle$ and $|1\rangle$ are represented by a sphere of radius 1, the so-called *Bloch Sphere* (see Figure 1), with $\theta \in [0, \pi]$ being the angle that the vector make with the vertical axis (z) and $\phi \in [0, 2\pi]$ being the angle that make the projection of vector in plane $x-y$. Defining a point in the sphere, then a qubit is represented on a sphere. The changes in this qubit are represented by rotations in this sphere.

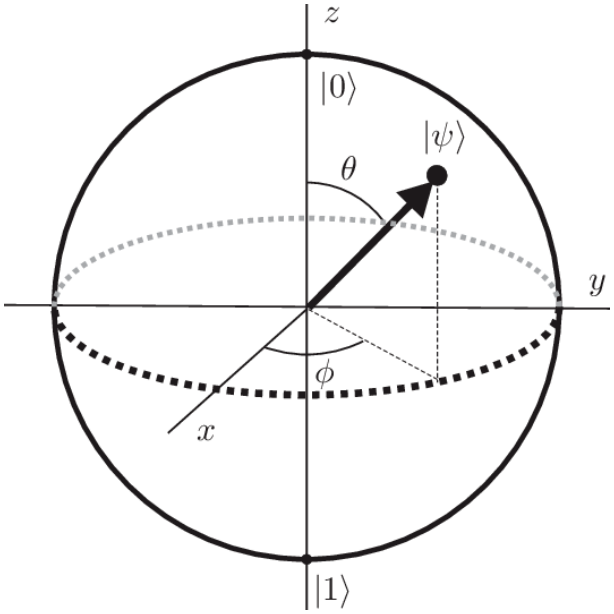

Figure 1 – The Bloch Sphere is a geometrical representation of the state space of a single qubit.

2.3 DENSITY MATRIX

We are able to describe the quantum system using density operator representation, the so-called *density matrix*, that provides an efficient description of quantum systems. The state of the system can be fully described by

$$\rho = \sum_i p_i |\psi_i\rangle \langle\psi_i| , \tag{2}$$

i.e, the state $|\psi_i\rangle$ with probability p_i.

A quantum system $|\psi\rangle$ that can be known in the exact way is called *pure state*. In this case, the density operator can be writing as $\rho = |\psi\rangle \langle\psi|$, that is when you know exactly which state vector the state is in. In the other way, ρ is called *mixed state* or a mixture of different pure states in the ensemble of ρ.

The operator ρ is a density operator associated with some ensemble $\{p_i, |\psi_i\rangle\}$ if and only if it meets the following conditions:

1. **Trace condition** — ρ has trace (the sum of diagonal elements) equal to one

$$tr(\rho) = \sum_i p_i tr(|\psi_i\rangle \langle\psi_i|) = \sum_i p_i = 1.$$

2. **Positivity condition** — ρ is a positive operator

$$\langle\Omega| \rho |\Omega\rangle = \sum_i p_i \langle\Omega|\psi_i\rangle \langle\psi_i|\Omega\rangle = \sum_i p_i |\langle\Omega|\psi_i\rangle|^2 \geq 0.$$

For pure states the density matrix also satisfies the following properties:

- $\rho^2 = \rho$,
- $tr(\rho^2) = 1$.

2.3.1 Reduced density operator

If ρ is the density operator that describes the AB composite system, then you can assign a density operator that describes the state of system A, called the reduced density operator, by $\rho_A = tr_B(\rho)$. Similarly, you can define ρ_B, the reduced density operator for system B. The tr_B operation is the partial trace on system B.

Bipartite system: let $|i_A\rangle$ and $|j_B\rangle$ be orthonormal basis for H_A e H_B (subsystems), so a density operator can be written in this basis as

$$\rho = \sum_{i,i',j,j'} \lambda_{i,i',j,j'} |i_A\rangle \langle i'_A| \otimes |j_B\rangle \langle j'_B|$$

so that,

$$tr_B(\rho) \equiv \sum_l \langle l_B| \rho |l_B\rangle$$

$$= \sum_l \langle l_B| \left(\sum_{i,i',j,j'} \lambda_{i,i',j,j'} |i_A\rangle |j_B\rangle \langle i'_A| \langle j'_B| \right) |l_B\rangle$$

$$= \sum_l \sum_{i,i',j,j'} \lambda_{i,i',j,j'} |i_A\rangle \langle l_B|j_B\rangle \langle i'_A| \langle j'_B|l_B\rangle .$$

Remembering that $\langle i|j\rangle = \delta_{ij}$, then

$$tr_B(\rho) = \sum_l \sum_{i,i'} \lambda_{i,i',l} |i_A\rangle \langle i'_A| .$$

2.3.2 Purity

The purity of a density operator measures the degree of mixedness of an arbitrary d-dimensional state and is described by

$$P(\rho) = tr(\rho^2), \tag{3}$$

which satisfies $1/d \leq P(\rho) \leq 1$, with the $1/d$ and 1 corresponding, respectively, to a fully mixed state and a pure state.

2.4 QUANTUM CIRCUITS

A quantum computer is a quantum machine set up to use QM to solve determined problems that a classical computer can not realize with the laws of Classical Physics. As discussed in the previous section, we have different computational models to perform

quantum computation. Here, we use the quantum circuit language defined by Deutsch (DEUTSCH, D., 1985; DEUTSCH, D. E., 1989).

In this section, we explore some quantum gates and measurement operations used in quantum circuits. The quantum logic gates are represented by unitary matrices so that a gate that acts in n qubits is represented by 2^nx2^n unitary matrix.

2.4.1 Single-qubit gates

The single qubit-gate performs a unitary operation U on an initial state $|\psi\rangle$ that evolves to $U|\psi\rangle$. A square matrix U is unitary if $U^\dagger U = UU^\dagger = I$, where $U^\dagger$ are the transpose conjugate of U, and consequently $|det(U)| = 1$. We can write any arbitrary 2x2 unitary matrix as

$$U = e^{i\alpha} R_{\hat{n}}(\theta), \tag{4}$$

where α and θ are real numbers, $\hat{n} = (x, y, z)$ is a real three-dimensional unitary vector, and the rotation operator, is defined by

$$R_{\hat{n}}(\theta) \equiv e^{-i\frac{\theta}{2}\hat{n}.\vec{\sigma}} = \cos\left(\frac{\theta}{2}\right) I - i \sin\left(\frac{\theta}{2}\right) \hat{n}\cdot\vec{\sigma}$$

where $\vec{\sigma} = (\sigma_X, \sigma_Y, \sigma_Z)$ denotes the three component vector of Pauli matrices.

Since the rotation operator can be decomposed according to the Euler's angles, a general 2x2 unitary matrix can be rewritten as

$$U = e^{i\alpha} R_x(\beta) R_y(\gamma) R_z(\delta)$$

$$= e^{i\alpha} \begin{bmatrix} e^{-i\beta/2} & 0 \\ 0 & e^{i\beta/2} \end{bmatrix} \begin{bmatrix} \cos\frac{\gamma}{2} & -\sin\frac{\gamma}{2} \\ \sin\frac{\gamma}{2} & \cos\frac{\gamma}{2} \end{bmatrix} \begin{bmatrix} e^{-i\delta/2} & 0 \\ 0 & e^{i\delta/2} \end{bmatrix}. \tag{5}$$

Below are shown some quantum single-gates and its circuit representation. The quantum gates X (that corresponding to the classical gate *NOT* or *bit-flip*), Y, and Z (that is a special case of a phase shift gate)

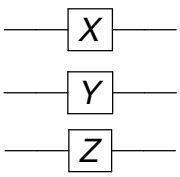

Their action is to perform a π rotation on the Bloch sphere around the $\hat{x}$, $\hat{y}$ and $\hat{z}$ axes, respectively

$$X|0\rangle = \begin{bmatrix} 0 & 1 \\ 1 & 0 \end{bmatrix} \begin{bmatrix} 1 \\ 0 \end{bmatrix} = |1\rangle, \quad X|1\rangle = \begin{bmatrix} 0 & 1 \\ 1 & 0 \end{bmatrix} \begin{bmatrix} 0 \\ 1 \end{bmatrix} = |0\rangle,$$

$$Y|0\rangle = \begin{bmatrix} 0 & -i \\ i & 0 \end{bmatrix} \begin{bmatrix} 1 \\ 0 \end{bmatrix} = i|1\rangle, \quad Y|1\rangle = \begin{bmatrix} 0 & -i \\ i & 0 \end{bmatrix} \begin{bmatrix} 0 \\ 1 \end{bmatrix} = -i|0\rangle,$$

$$Z|0\rangle = \begin{bmatrix} 1 & 0 \\ 0 & -1 \end{bmatrix} \begin{bmatrix} 1 \\ 0 \end{bmatrix} = |0\rangle, \quad Z|1\rangle = \begin{bmatrix} 1 & 0 \\ 0 & -1 \end{bmatrix} \begin{bmatrix} 0 \\ 1 \end{bmatrix} = -|1\rangle.$$

The action of the Hadamard quantum gate H results in a superposition of states and is represented by

$$H = \frac{1}{\sqrt{2}} \begin{bmatrix} 1 & 1 \\ 1 & -1 \end{bmatrix}.$$

It is just a rotation about the $\hat{y}$ axis by $\frac{\pi}{2}$, followed by a rotation about the $\hat{x}$ axis by π,

$$H|0\rangle = \frac{1}{\sqrt{2}}(|0\rangle + |1\rangle) \quad \text{and} \quad H|1\rangle = \frac{1}{\sqrt{2}}(|0\rangle - |1\rangle).$$

Others quantum single-gates are the identity and phase shift gates

$$I = \begin{bmatrix} 1 & 0 \\ 0 & 1 \end{bmatrix}, \quad R_\vartheta = \begin{bmatrix} 1 & 0 \\ 0 & e^{i\vartheta} \end{bmatrix},$$

where ϑ is the phase shift.

2.4.2 Two-qubit gates

A basic two qubit gate is the *controlled-not* gate or *CNOT*, that can be represented as

$$CNOT = \begin{bmatrix} 1 & 0 & 0 & 0 \\ 0 & 1 & 0 & 0 \\ 0 & 0 & 0 & 1 \\ 0 & 0 & 1 & 0 \end{bmatrix},$$

with the first qubit being called *control qubit* and the second the *target qubit*. We can interchange the control qubit, the first qubit as a target qubit and second as a control qubit. The control bit does not change, while the target bit flips if and only if the control bit is in state $|1\rangle$. The circuital representation of a controlled-gate is

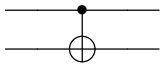

More generally, if U is some single-qubit gate, then the 2-qubit *controlled* $-U$ gate corresponds to the following 4x4 unitary matrix

$$\begin{bmatrix} 1 & 0 & 0 & 0 \\ 0 & 1 & 0 & 0 \\ 0 & 0 & U_{11} & U_{12} \\ 0 & 0 & U_{21} & U_{22} \end{bmatrix},$$

that is circuit represented by

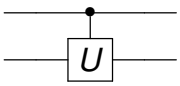

2.4.3 Measurement

Measurement is not a unitary operation, because it takes a quantum state and projects it into one of the measurement operator eigenstates, the state collapses to a definitive single value. Its circuit representation is

2.5 ENTROPY

Entropy is a concept approached in Statistical Physics and can be obtained using the information theory. Here we explore this tool to quantify the quantum correlations. We cover in this chapter the classical (Shannon) and quantum (von Neumann) entropy.

2.5.1 Shannon Entropy

In the Classical Theory of Information, the Shannon entropy (SHANNON, 1948) can be interpreted as the uncertainty associated to a random variable A with a probability distribution $\{p_a\}$. It is defined by

$$H(A) = -\sum_{a \in A} p_a \log_2 p_a,$$

where p_a is that probability that A assume the value a. The joint entropy associated to two random variables A and B is described by

$$H(A,B) = -\sum_{a \in A, b \in B} p_{a,b} \log_2 p_{a,b},$$

with $p_{a,b}$ being the probability of A assume the value a and B assume the value b. The joint entropy measure our total uncertainly about the pair of random variables. There is also the conditional entropy, which is written as

$$H(A|B) \equiv H(A,B) - H(B), \tag{6}$$

where we used $\sum_a p_{a,b} = p_b$ and the Bayes's rule $p_{a|b} = \frac{p_{a,b}}{p_b}$ to derive this expression. Then, the conditional entropy is a measure of the average uncertainty about the value of A, given that we know the value of B. The total correlations between these two variables A and B is measured by mutual information, given by

$$H(A:B) \equiv H(A) + H(B) - H(A,B), \tag{7}$$

that measures how much information these variables have in common.

2.5.2 Von Neumann Entropy

In the quantum scenario, the information of a physical system is stored in the quantum states that are described by density operators, that are hermitian and positive semidefinite. The eigenvalues of ρ compose a distribution of probability. So, the quantum analog of Shannon entropy is described by the von Neumann entropy

$$S(\rho) = -Tr(\rho \log_2 \rho). \tag{8}$$

Von Neumann entropy is a quantifier of the number of orthonormal pure states accessible from the system. For mixed states, this measure fails to distinguish classical and quantum mechanical correlations (VEDRAL et al., 1997). For pure states $S(\rho) = 0$ (complete information about the system, since the state is well-defined) and for statistical mixtures $S(\rho) \neq 0$.

Here we use the reference (ROSSATTO et al., 2014). To make the analog of classical mutual information (eq. 7) for a bipartite quantum system with density operator ρ^{AB} we use the von Neumann entropy, leading to the expression

$$I(\rho^{AB}) = S(\rho^A) + S(\rho^B) - S(\rho^{AB}), \tag{9}$$

where $S(\rho^A)$ and $S(\rho^B)$ are the entropy of subsystems A and B, respectively, calculated using partial trace with respect to the other subsystem $\rho^A = Tr_B(\rho^{AB})$ and $\rho^B = Tr_A(\rho^{AB})$. However, the quantum version of expression 2.6 is not easily obtained because the Bayes rule is not always valid in the quantum case. Since the measurement process can be done in different ways and it can disturb the system, we have that the conditional entropy is given by

$$S(\rho^{A|B}) = min_{\epsilon_b} \sum_b p_b S(\rho^{A|B=b}),$$

where $\rho^{A|B=b} = \frac{Tr_B(I_A \otimes \epsilon_b \rho^{AB})}{Tr(I_A \otimes \epsilon_b \rho^{AB})}$, with ϵ_b being a measurement set on the subsystem B. Then, we can define the quantum analogue of eq. 6 as

$$J(\rho^{AB}) = S(\rho^A) - min_{\epsilon_b} \sum_b p_b S(\rho^{A|B=b}). \tag{10}$$

3 QUANTUM CORRELATIONS

Correlation in a composite system is a fundamental concept in Quantum Information Theory. The information that can be derived from nature is determined by how much the system of interest can be correlated by physics interaction with the measurement apparatus. Quantum Correlations are essential resources for Quantum Information and Computation (ADESSO; BROMLEY; CIANCIARUSO, 2016), Communication (TUFARELLI et al., 2012), Cryptography (CURTY et al., 2005), and Quantum Metrology (MODI; CABLE, et al., 2011).

The study of Quantum Correlations began with the development of Quantum Theory. One of the most prominent articles was 1935 in which Einstein, Podolsky, and Rosen (EINSTEIN; PODOLSKY; ROSEN, 1935) argued that a physical theory should satisfy the following properties:

1. *Realism* — An element of reality is an amount that can be obtained with certainty without disturbing the system;

2. *Completeness* — Each element of reality must be described by an object of the theory;

3. *Locality* — Physical processes occurring in one place should not have an immediate effect on reality elements elsewhere.

According to these properties, the Quantum Theory has been proven not to be complete as it does not satisfy all properties at the same time. If realism and locality are introduced in QM we get a contradiction.

We could ask if there are variables that completely describe QM. These variables would be called hidden variables, since we do not have access to them. If these hidden variables exist, they should be a local theory to prevent interactions and communication at distance. A local hidden variable model must be able to reproduce all predictions of QM satisfying all the properties at the same time.

3.1 BELL'S NONLOCALITY

John Bell in 1964 (BELL, 1964) showed that using the superposition principle applied to compound systems produces quantitative predictions which, if confirmed experimentally, expose non-local aspects of QM. He propose that the conditions of realism, completeness and locality impose that spatially separated statistical correlations must satisfy some conditions known as Bell's inequalities. Contrary to the expectations, these inequalities are violated by some entangled states, this condition is known as *Nonlocality*. It was shown experimentally first by Aspect in 1982 that QM is not locally realistic

(ASPECT; GRANGIER; ROGER, 1982) and only in 2015 we had an experiment without loophole that demonstrates its non-local character (HENSEN et al., 2015).

Local Realism — It is hypothesized that physical objects have defined properties that are independent of the observation process and that a measurement made by one observer can not influence measurements made by another observer if they are so separated that the exchange of information between them is impossible with Special Relativity.

Bell's theorem establishes that there is a conflict between the QM and the theory of hidden variables. The Bell's inequalities must be obeyed by any Local Realistic Theory. QM is incompatible with any theory of local hidden variables.

The Bell's inequalities can be used in quantum cryptography to test its security (EKERT, 1991). Every pure entangled state violates some Bell's inequality (GISIN, 1991). For mixed states, a necessary and sufficient condition for any two-qubit state to violate these inequalities is given by Horodecki et al. (HORODECKI; HORODECKI; HORODECKI, 1995).

Bell's inequality via CHSH— For two qubits systems, the Clause-Horne-Shimony-Holt (CHSH) inequality (CLAUSER et al., 1969) is the most known type of Bell's inequality. There are different ways in literature to derive such inequality. Here we use the reference (BALLENTINE, 2014) and (BRAUNSTEIN; CAVES, 1990). We assume a system where Alice and Bob have experimental apparatus with orientations a and b, respectively, capable of measuring the variables A and B that can assume the values ± 1. According to local realism, the measurement made by Alice can not depend on the orientation chosen by Bob and vice versa, so the possible results of the measures depend only on the hidden variable λ and the orientation chosen by each one

$$A(a,\lambda) = \pm 1,$$
$$B(b,\lambda) = \pm 1.$$

We can define the correlation function given by

$$C(a,b) = \int A(a,\lambda)B(b,\lambda)\rho(\lambda)d\lambda$$

where $\rho(\lambda)$ is the probability distribution of the hidden variable and must satisfy the conditions

- $\rho(\lambda) \geq 0$,
- $\int \rho(\lambda)d\lambda = 1$.

Now, considering that Alice and Bob can randomly choose two orientations each a, a' and b, b', respectively, we have four correlations functions that must satisfy the inequality

$$B = |C(a,b) - C(a,b')| + (C(a',b') + C(a',b)) \leq 2.$$

If a composite system violates the above inequality, we say that it does not satisfy Bell's locality hypothesis.

3.1.1 Bell's nonlocality quantifier

Any two-qubit state can be parameterized via the Fano matrix (FANO, 1983) as

$$\rho^{AB} = \frac{1}{4}\left(I^A \otimes I^B + I^A \otimes (\vec{\sigma}^B \cdot \vec{r}) + (\vec{\sigma}^A \cdot \vec{s}) \otimes I^B + \sum_{i,j=1}^{3} c_{ij} \vec{\sigma}_i{}^A \otimes \vec{\sigma}_j{}^B \right), \tag{11}$$

where $\vec{\sigma}^A = (\sigma_x^A, \sigma_y^A, \sigma_z^A)$ and $\vec{\sigma}^B = (\sigma_x^B, \sigma_y^B, \sigma_z^B)$ are the Pauli matrices,

$$\vec{r} = tr[\rho(I_A \otimes \vec{\sigma}^B)] \quad \text{and} \quad \vec{s} = tr[\rho(\vec{\sigma}^A \otimes I_B)]$$

are called polarization vectors, and $c_{ij} = tr[\rho(\vec{\sigma}_i{}^A \otimes \vec{\sigma}_j{}^B)]$ are the elements of the correlation matrix C. We define the matrix $T = C \cdot C^T$, with m_1 and m_2 being the two largest eigenvalues of T. As demonstrated by Horodecki et al. (HORODECKI; HORODECKI; HORODECKI, 1995), the quantity defined below

$$B(\rho^{AB}) = 2\sqrt{m_1 + m_2}, \tag{12}$$

is $B(\rho^{AB}) \leq 2$ if the Bell's inequality is not violated, otherwise, non-local effects appear. The violation occurs only if $(m_1 + m_2) > 1$, i.e., if the quantum state produces $B(\rho) > 2$ we guarantee that this state violates inequality and has non-local characteristics. This measure will be used to obtain the correlations for the studied model.

3.2 ENTANGLEMENT

Entanglement is a fundamental characteristic of QM that is used for processing and transmission of QI and it is employed during the performing tasks as teleportation protocol (VAIDMAN, 1994). This correlation is related to the superposition principle (section 2.1). Werner (WERNER, 1989) showed that there are entangled mixed state that do not violate Bell's inequalities. Entanglement is considered a quantifier of purely quantum correlations of a state.

Here we use the reference (PASSANTE, 2012),

- A pure state is entangled if and only if it is not a product state written in the form

$$|\psi_{AB}\rangle = |\psi_A\rangle \otimes |\psi_B\rangle .$$

- Any state ρ is entangled if and only if it can not be expressed as a convex combination of product states of all subsystems that form the composite system

$$\rho \neq \sum_i p_i \rho_i^{(1)} \otimes \rho_i^{(2)} \cdots \otimes \rho_i^{(n)},$$

with

$$\sum_i p_i = 1.$$

All non-entangled states are called separable. Entanglement is defined as the non-separability of a quantum state. Classical states are states that can be generated via Local Operations and Classical Communication (LOCC). Local Operations refer to operations performed only on one part of the system. Classical Communication refers to the transmission of information using classical devices. If a state can not be generated through LOCC it is non-separable resulting in entangled.

3.2.1 Entanglement measure

For pure states, the von Neumann entropy is used to quantify the entanglement of a quantum system. For this, we call the entanglement entropy which is described in terms of the entropy of the reduced system density matrix

$$E(\rho) = S(\rho_A) = -\sum_i \lambda_i \log_2 \lambda_i,$$

where λ_i are the eigenvalues of ρ_A,

- $E(\rho) = 0$ for separable states, and
- $0 < E(\rho) \leq \log_2 D$ for entangled states, where D is the dimension of subsystem. If the state has $E(\rho) = \log_2 D$, it is said maximally entangled,

(BENGTSSON; ZYCZKOWSKI, 2006).

For an entanglement measure to be appropriate, it must meet the conditions shown in reference (COSTA, 2012).

The Peres-Horodecki or PPT (*positive partial transpose*) criterion, that is based on partial transposition of the density matrix, is a necessary and sufficient condition to evaluate if a state is entangled. If we have a density matrix that can be written in separable form (PERES, 1996; HORODECKI, 1997; SIMON, R., 2000),

$$\rho^{AB} = \sum_i p_i \rho_{A,i} \otimes \rho_{B,i},$$

the partial transposition modify only one of the subsystems A or B, leaving the other unchanged. This criterion shows that if partial transposition of the density matrix results in negative eigenvalues, then the systems partitions are entangled.

We have a family of norms parameterized by a real number $p \geq 1$, called *Schatten p-norms*, that are defined as

$$\|A\|_{(p)} = \{tr[(A^\dagger A)^{p/2}]\}^{1/p}, \tag{13}$$

obtaining a singular value of a matrix A. In particular, we use the 1-norm, also called trace norm, and the 2-norm, also called Hilbert-Schmidt norm (NAKANO; PIANI; ADESSO, 2013).

Vidal and Werner (VIDAL; WERNER, 2002) define the *negativity* of a bipartite system as

$$N(\rho) = \frac{\|\rho^{T_A}\|_1 - 1}{2}, \tag{14}$$

which corresponds to the absolute value of the sum of negative values of the partial transpose of the state ρ, in other words, we have the trace norm (see eq. 13) of ρ^{T_A}, that is a partial transposition in subsystem A (we can also define partial transposition for subsystem B). The negativity can assume values between 0 and $(d-1)/2$, where d is the minimum between the partition dimensions A and B. This expression for negativity corresponds to how far the partial trace of the density matrix is from positive, and consequently, the amount of entanglement between the subsystems. Eq. 14 will be used to quantify entanglement in the DQC1 model.

3.3 QUANTUM DISCORD

With independent research Henderson & Vedral (HENDERSON; VEDRAL, 2001) and Zurek & Ollivier (OLLIVIER; ZUREK, 2001) found that there are quantum correlations that are not quantified only by entanglement or nonlocality. These correlations became known as *Quantum Discord*, which is defined in terms of the generalization of the concept of mutual information in quantum systems (see eq. 8 and eq. 9) (MAZIERO; CELERI; SERRA, 2010), (MODI; BRODUTCH, et al., 2012),

$$\begin{aligned} D(\rho^{AB}) &\equiv I(\rho^{AB}) - J(\rho^{AB}) \\ &= S(\rho^B) - S(\rho^{AB}) + min_{\epsilon_b}(\sum_b p_b S(\rho^{A|B=b})), \end{aligned}$$

where the measurement is performed on the subsystem B. So, discord is a measure of information that can not be extracted locally. This minimization process is designed so that the quantum discord does not depend on the choice of the measurement projector set.

For almost all separable states the quantum discord value found is nonzero, just as almost all pure states possess entanglement (FERRARO et al., 2010), (CAVALCANTI et al., 2011). For pure states, quantum discord is reduced to entanglement. Considering all two-qubit states, the quantum discord satisfies

$$0 \leq D(\rho^{AB}) \leq 1.$$

Dakic et al. (DAKIĆ; VEDRAL; BRUKNER, 2010) propose a geometric measure of quantum discord, which is the distance from the analyzed state ρ to the nearest Classical-Quantum state χ (or with zero discord)

$$D(\rho) = min_{\chi\in\Omega}\|\rho-\chi\|^2,$$

where Ω is the zero-discord state set and $\|\rho-\chi\|^2 = Tr(\rho-\chi)^2$ is the square of the Hilbert-Schmidt norm (see eq. 13).

3.3.1 Quantum discord for two-qubit systems

Dakic et al. (DAKIĆ; VEDRAL; BRUKNER, 2010) provided a closed form for the expression of the geometric discord of arbitrary two-qubit states

$$D(\rho) = \frac{1}{4}\left(\|\vec{s}\|_2^2 + \|C\|_2^2 - \lambda_{max}\right), \tag{15}$$

where C is calculated using the square of the Hilbert-Schmidt norm (see eq. 13), $\vec{s}$ using the euclidean norm given by

$$||\vec{s}||_2 = \left(\sum_{i=1}^{n}|s_i|^2\right)^{1/2}.$$

Using the parameterization described in eq. 11, with $\vec{s}$ the polarization vector and the correlation matrix C, λ_{max} represents the largest eigenvalue of the matrix

$$\Lambda = \vec{s}\cdot\vec{s}^T + C\cdot C^T.$$

Any state of two qubits can be decomposed into the above form via local unitary operations (which by definition preserve entanglement and correlations in general). Expression 15 is valid for states with dimension 2xd (RAU et al., 2011).

3.4 COHERENCE

To investigate the physical meaning of the density matrix elements, we have to explore concepts such as populations and coherence. Here we use the reference (ARRUDA, 2011). To explore concept of coherence, it is necessary to study the elements outside the diagonal of the density matrix ρ. For mixed states, the density matrix can be written as eq. 2, and assuming an orthogonal basis $\{|\zeta_l\rangle\}$, i.e. $\langle\zeta_k|\zeta_l\rangle = \delta_{k,l}$, we can write the elements outside the diagonal of the density matrix as

$$\begin{aligned}\rho_{m,n} &= \langle\zeta_m|\rho|\zeta_n\rangle \\ &= \sum_i p_i \langle\zeta_m|\psi_i\rangle\langle\psi_i|\zeta_n\rangle = \sum_i p_i c_m^i c_n^{i*},\end{aligned}$$

where c_m^i are the $|\psi_i\rangle$ components at the base $|\zeta_m\rangle$, and c_n^{i*} are the $|\psi_i\rangle$ components at the base $|\zeta_n\rangle$, they are express the effects of interference between $|\zeta_m\rangle$ and $|\zeta_n\rangle$ states. If $\rho_{m,n}=0$ means that the projections on $|\zeta_m\rangle$ and $|\zeta_n\rangle$ states have been canceled, and if $\rho_{m,n}\neq 0$ there is a certain coherence between $|\zeta_m\rangle$ and $|\zeta_n\rangle$ states.

Coherence measures must satisfy some conditions, as shown in Braumgratz et al. (BAUMGRATZ; CRAMER; PLENIO, 2014). We can have a measure of coherence based on quantum relative entropy (ABERG, 2006), (BAUMGRATZ; CRAMER; PLENIO, 2014) described as

$$C_{rel.ent.}(\rho) = S(\rho_{diag}) - S(\rho),$$

where S is the von Neumann entropy and ρ_{diag} denotes the state obtained from ρ by deleting all off-diagonal elements. There is another measure of coherence based on l_1 norm (HORN; JOHNSON, 2012)

$$C_{l_1}(\rho) = \sum_{i\neq j} |\rho_{i,j}|,$$

that is the sum of the absolute values of all off-diagonal elements of the density matrix ρ. For the one-qubit case $C_{l_1}(\rho)$ has the same form of the trace norm (SHAO et al., 2015). Then we can use the trace norm as a measure coherence

$$C(\rho) = \|\rho - \rho_{diag}\|_1, \tag{16}$$

(YU et al., 2016).

Quantum coherence is a basis-dependent quantity, so even local unitary transformations can increase quantum coherence in two-part systems. It is not like entanglement and quantum discord that are invariant about the product of local unitary transformations.

3.5 QUANTUM CORRELATIONS FOR THE WERNER STATE

To illustrate an example using the measurement of correlations, Figure 2 shows the normalized measures of correlations

$$\begin{gathered} B_N(\rho) = B(\rho)/2\sqrt{2}, \quad C_N(\rho) = C(\rho)/3.0, \\ D_N(\rho) = D(\rho)/0.5, \quad N_N(\rho) = N(\rho)/0.5, \end{gathered} \tag{17}$$

for a Werner's state given by

$$\rho_W = \frac{(1-q)}{4} I + q\,|\Phi^+\rangle\langle\Phi^+|, \tag{18}$$

where $|\Phi^+\rangle = \frac{1}{\sqrt{2}}(|00\rangle + |11\rangle)$ is one of the Bell state. The figure shows that for $q > 1/3$ we have entangled states, and for $q \leq 1/3$ we have separable states. Then for $q > \sqrt{2}/2$ we have Bell violation. For the state with $q = 1$, the Bell's nonlocality, quantum discord, and negativity normalized quantities reach the maximum value of 1.

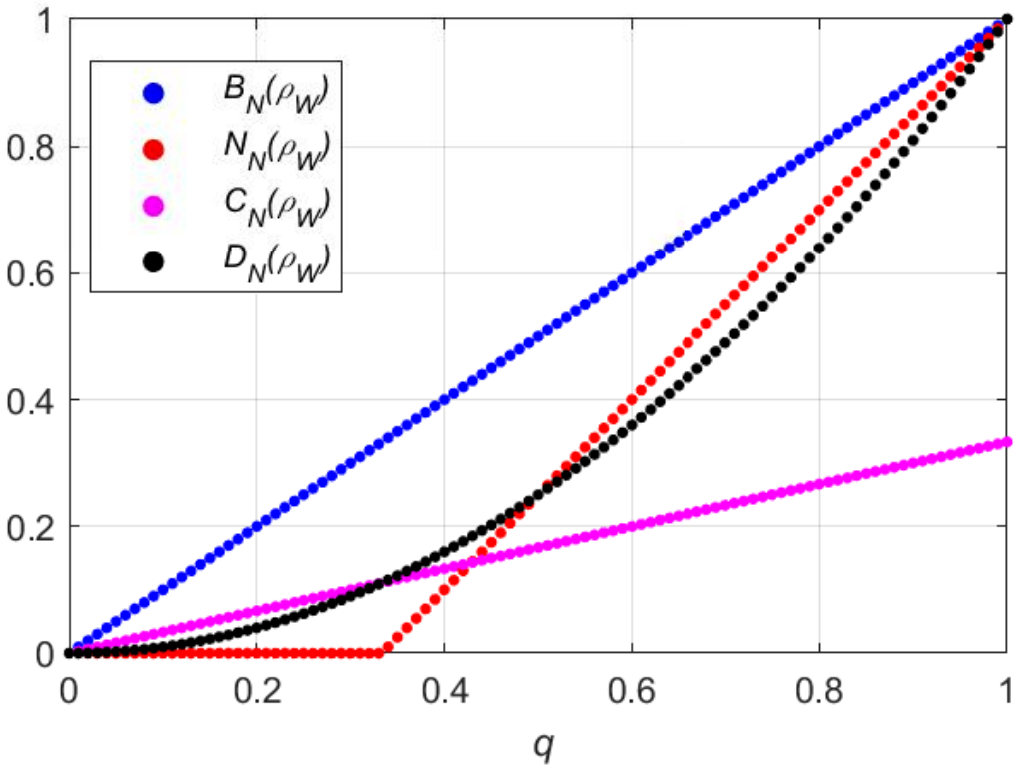

Figure 2 – Normalized quantum correlations for the Werner state.

4 DETERMINISTIC QUANTUM COMPUTATION WITH ONE QUBIT

Deterministic Quantum Computation with One Qubit (DQC1) is a model of computation that efficiently performs the normalized trace of any unitary operator and was introduced in 1998 by (KNILL; LAFLAMME, 1998). Once this model evaluates efficiently the normalized trace of any unitary matrix, the idea is to be able to code certain problems in the problem of calculating the trace of a unitary matrix. The advantage that this model presents in relation to its classical counterpart is due to the fact that to calculate the trace of a unitary matrix with the classical computation it is necessary to add the elements of the diagonal and as the dimension of this unitary matrix increases, this calculation becomes more difficult to be executed (DATTA, 2008). This model is not universal, but presents an advantage in comparison with certain problems using classical algorithms. Some of these problems were studied in literature, such as Shor Factorization (PARKER; PLENIO, 2000), Estimate Jones Polynomials (SHOR; JORDAN, 2007), Measure the Average Fidelity Decay (POULIN et al., 2004), and Estimate Parameters at the Quantum Metrology Limit (BOIXO; SOMMA, 2008). The importance of this model is due to the fact that it requires no entanglement between A and B (control and auxiliary) to perform the operation (DATTA; FLAMMIA; CAVES, 2005).

The DQC1 circuit (shown in Figure 3) consists of an input qubit with a certain degree of coherence α and the n others in the total statistical mixture. The computation is performed applying a controlled unitary quantum gate between the control and auxiliary qubits, and the result is obtained measuring the first qubit (SANTOS et al., 2015). The

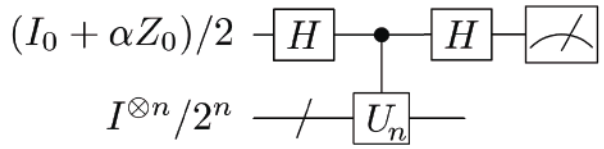

Figure 3 – DQC1 circuit applied to evaluate the normalized trace of a unitary matrix. The control qubit is a semi-pure state while the n auxiliary qubits are in the maximum mixture state.

control qubit is initialized in the state $\rho_0(\alpha) = \frac{(I_0+\alpha Z_0)}{2}$ (semi-pure state) with $0 \leq \alpha \leq 1$. While the other n qubits are initialized in state $\rho_n = \frac{I^{\otimes n}}{2^n}$. The total initial state of the system is

$$\rho_i = \frac{(I_0 + \alpha Z_0)}{2} \otimes \frac{I^{\otimes n}}{2^n},$$

where the index "0" refers to the control qubit, I represents the identity matrix, $Z = \sigma_Z$ for one qubit, and $I^{\otimes n}$ is the identity matrix of the n qubits.

We perform the following computational steps

1. Apply the Hadamard gate on the initial state

$$H_0 \rho_i H_0^\dagger = \frac{1}{2^{n+1}} [(|0\rangle\langle 0| + |1\rangle\langle 1|) + \alpha(|0\rangle\langle 1| + |1\rangle\langle 0|)] \otimes I^{\otimes n}.$$

2. Apply a controlled unitary gate,

$$U = |0\rangle\langle 0| \otimes I^{\otimes n} + |1\rangle\langle 1| \otimes U_n,$$

between the control and auxiliary qubits, followed by the Hadamard gate, resulting in the state

$$\begin{aligned} \rho_f &= (H_0 \otimes I^{\otimes n}) U H_0 \rho_i H_0^\dagger U^\dagger (H_0^\dagger \otimes I^{\otimes n}) \\ &= \frac{1}{2^{n+1}} \begin{bmatrix} I_{n+1} & \alpha U^\dagger{}_n \\ \alpha U_n & I_{n+1} \end{bmatrix}. \end{aligned}$$

3. Finally, we measure σ_x and σ_y in the control qubit, obtaining

$$\begin{aligned} \langle \sigma_x \rangle = tr(\rho_f \sigma_x) &= \frac{1}{2^{n+1}} \begin{bmatrix} tr(\alpha U^\dagger{}_n) & tr(I_{n+1}) \\ tr(I_{n+1}) & tr(\alpha U_n) \end{bmatrix} \\ &= \frac{\mathbb{R}[tr(\alpha U_n)]}{2^n}, \end{aligned}$$

and

$$\begin{aligned} \langle \sigma_y \rangle = tr(\rho_f \sigma_y) &= \frac{1}{2^{n+1}} \begin{bmatrix} tr(i\alpha U^\dagger{}_n) & tr(-iI_{n+1}) \\ tr(iI_{n+1}) & tr(-i\alpha U_n) \end{bmatrix} \\ &= \frac{\mathbb{I}_m[tr(\alpha U_n)]}{2^n}, \end{aligned}$$

where $\mathbb{R}$ and $\mathbb{I}_m$ stands for the real and imaginary parts, respectively. To promote other correlations in this computation model, we introduced a specific post-selection after the circuit. This post-selection acts through a filter described by (KENT; LINDEN; MASSAR, 1999). Finding physical resources responsible for the advantage of quantum computing over classical computing is an active research topic (PASSANTE et al., 2011), (DATTA; SHAJI; CAVES, 2008), (DATTA; FLAMMIA; CAVES, 2005), (LANYON et al., 2008). Following this line, it has been shown that the amount of entanglement present at the end of the DQC1 computation process, i.e. the evaluation of the normalized trace of a unitary matrix, is not enough to explain the resulting computational gain (DATTA; VIDAL, 2007), (DATTA; FLAMMIA; CAVES, 2005), (DAKIĆ; VEDRAL; BRUKNER, 2010). However, there are other QC beyond entanglement that encompass this correlation that could account for this advantage, such as quantum discord (DATTA; SHAJI; CAVES, 2008). As presented in the previous chapter, the correlations of entanglement, Bell's nonlocality, quantum discord, and coherence present closed forms for the calculation with two qubits, we will write our model with two qubits (control and auxiliary) to analyze these correlations.

4.1 TWO-QUBITS SYSTEM

Since we have measures of quantum correlations with closed form for two-qubits introduced in section 3, we chose to analyze this scenario first. Then, for $n=1$, a general unitary matrix acting on states of one qubit described by eq. 5 can be written as

$$U_{n=1} = e^{i\frac{\varphi}{2}} \begin{bmatrix} e^{i\psi} & 0 \\ 0 & e^{-i\psi} \end{bmatrix} \begin{bmatrix} \cos\theta & \sin\theta \\ -\sin\theta & \cos\theta \end{bmatrix} \begin{bmatrix} e^{i\Delta} & 0 \\ 0 & e^{-i\Delta} \end{bmatrix}.$$

As we want to write the expressions for $\vec{s}$, $\vec{r}$, and C, we initialize the control qubit in an arbitrary state $\rho_0 = \frac{I+\vec{u}\cdot\vec{\sigma}}{2}$. The final density matrix is

$$\rho_{final} = (H_0 \otimes I)\, U\, (H_0 \rho_0 H_0 \otimes \rho_{n=1})\, U^{\dagger} (H_0 \otimes I), \tag{19}$$

with $\rho_{n=1} = \frac{I}{2}$ for the auxiliary qubit. Therefore,

$$\begin{aligned}
\rho_{final} = {} & \frac{1}{2}|0\rangle\langle 0| \otimes \left(\frac{I}{2} + \frac{1}{4}(u_z + iu_y) U_{n=1}^{\dagger} + \frac{1}{4}(u_z - iu_y) U_{n=1} \right) \\
& + \frac{1}{2}|0\rangle\langle 1| \otimes \left(\frac{I}{2} u_x - \frac{1}{4}(u_z + iu_y) U_{n=1}^{\dagger} + \frac{1}{4}(u_z - iu_y) U_{n=1} \right) \\
& + \frac{1}{2}|1\rangle\langle 0| \otimes \left(\frac{I}{2} u_x + \frac{1}{4}(u_z + iu_y) U_{n=1}^{\dagger} - \frac{1}{4}(u_z - iu_y) U_{n=1} \right) \\
& + \frac{1}{2}|1\rangle\langle 1| \otimes \left(\frac{I}{2} - \frac{1}{4}(u_z + iu_y) U_{n=1}^{\dagger} - \frac{1}{4}(u_z - iu_y) U_{n=1} \right) \\
= {} & \frac{1}{4} \begin{bmatrix} a_{11} & a_{12} & a_{13} & a_{14} \\ a_{12}^* & a_{22} & a_{23} & a_{24} \\ a_{13}^* & a_{23}^* & a_{33} & a_{34} \\ a_{14}^* & a_{24}^* & a_{34}^* & a_{44}^* \end{bmatrix},
\end{aligned}$$

where the matrix elements are given by

$$a_{11} = 1+\cos\theta\left[u_z\cos(\Delta+\frac{\phi}{2}+\psi)+u_y\sin(\Delta+\frac{\phi}{2}+\psi)\right];$$
$$a_{12} = -ie^{-i(\Delta-\psi)}\sin\theta\left[u_y\cos\frac{\phi}{2}+u_z\sin\frac{\phi}{2}\right];$$
$$a_{13} = u_x - i\cos\theta\left[u_y\cos(\Delta+\frac{\phi}{2}+\psi)-u_z\sin(\Delta+\frac{\phi}{2}+\psi)\right];$$
$$a_{14} = -ie^{-i(\Delta-\psi)}\sin\theta\left[u_y\cos\frac{\phi}{2}+u_z\sin\frac{\phi}{2}\right];$$
$$a_{22} = 1+\cos\theta\left[u_z\cos(\Delta-\frac{\phi}{2}+\psi)-u_y\sin(\Delta-\frac{\phi}{2}+\psi)\right];$$
$$a_{23} = -e^{i(\Delta-\psi)}\sin\theta\left[u_z\cos\frac{\phi}{2}+u_y\sin\frac{\phi}{2}\right];$$
$$a_{24} = u_x - i\cos\theta\left[u_y\cos(\Delta-\frac{\phi}{2}+\psi)+u_z\sin(\Delta-\frac{\phi}{2}+\psi)\right];$$
$$a_{33} = 1-\cos\theta\left[u_z\cos(\Delta+\frac{\phi}{2}+\psi)+u_y\sin(\Delta+\frac{\phi}{2}+\psi)\right];$$
$$a_{34} = ie^{-i(\Delta-\psi)}\sin\theta\left[u_y\cos\frac{\phi}{2}+u_z\sin\frac{\phi}{2}\right];$$
$$a_{34} = ie^{-i(\Delta-\psi)}\sin\theta\left[u_y\cos\frac{\phi}{2}+u_z\sin\frac{\phi}{2}\right];$$
$$a_{44} = 1-\cos\theta\left[u_z\cos(\Delta-\frac{\phi}{2}+\psi)-u_y\sin(\Delta-\frac{\phi}{2}+\psi)\right].$$

Using the Fano's form, as eq. 11, to calculate the polarization vectors $\vec{r} = tr[\rho(I_A\otimes\vec{\sigma}^B)]$, $\vec{s} = tr[\rho(\vec{\sigma}^A\otimes I_B)]$, and the elements of correlation matrix C, $c_{ij} = tr[\rho(\vec{\sigma}_i{}^A\otimes\vec{\sigma}_j{}^B)]$, we obtain

$$\vec{r} = \begin{bmatrix}0\\0\\0\end{bmatrix},$$

$$\vec{s} = \begin{bmatrix} u_x \\ \cos\theta\cos(\Delta+\psi)\left(u_y\cos\frac{\phi}{2}-u_z\sin\frac{\phi}{2}\right) \\ \cos\theta\cos(\Delta+\psi)\left(u_z\cos\frac{\phi}{2}+u_y\sin\frac{\phi}{2}\right)\end{bmatrix},$$

and

$$C = \begin{bmatrix} c_{11} & c_{12} & c_{13} \\ c_{21} & c_{22} & c_{23} \\ c_{31} & c_{32} & c_{33}\end{bmatrix},$$

with

$$
\begin{aligned}
c_{11} &= c_{12} = c_{13} = 0; \\
c_{21} &= -\sin(\psi-\Delta)\sin\theta\left(u_z\cos\frac{\phi}{2}+u_y\sin\frac{\phi}{2}\right); \\
c_{22} &= -i\sin(\psi-\Delta)\sin\theta\left(u_z\cos\frac{\phi}{2}+u_y\sin\frac{\phi}{2}\right); \\
c_{23} &= -\sin(\psi+\Delta)\cos\theta\left(u_z\cos\frac{\phi}{2}+u_y\sin\frac{\phi}{2}\right); \\
c_{31} &= \sin(\psi-\Delta)\sin\theta\left(u_y\cos\frac{\phi}{2}+u_z\sin\frac{\phi}{2}\right); \\
c_{32} &= \cos(\psi-\Delta)\sin\theta\left(u_y\cos\frac{\phi}{2}+u_z\sin\frac{\phi}{2}\right); \\
c_{33} &= \sin(\psi+\Delta)\cos\theta\left(u_y\cos\frac{\phi}{2}-u_z\sin\frac{\phi}{2}\right).
\end{aligned}
$$

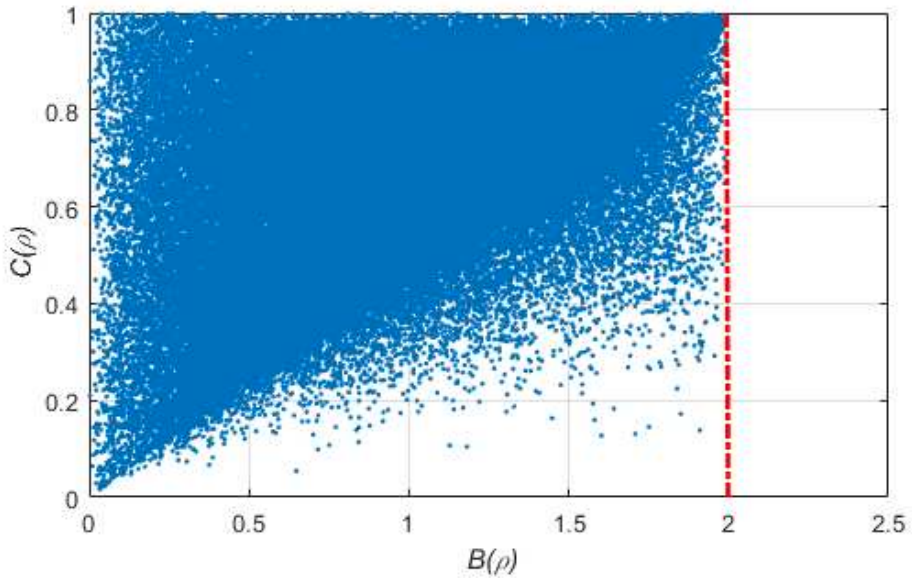

Figure 4 – $C(\rho)$ versus $B(\rho)$ for the DQC1 model with two qubits. Each dot represents the value of these correlations calculated for 10^6 random states. The red dotted line represents the limit value of $B(\rho)$ in which there is no Bell's nonlocality.

As expected for this model, there is no entanglement (DATTA; FLAMMIA; CAVES, 2005) between the control and the auxiliary qubits, as calculated by eq. 14 and consequently no Bell-violation, as calculated by eq. 12. Quantum Correlations plots for the DQC1 model with two qubits using 10^6 random unitary matrices drawn from Haar measure (ZYCZKOWSKI; KUS, 1994), (OZOLS, 2009) with a function called *RandomUnitary* in the QETLAB (can be obtained in `http://www.qetlab.com/`, that is a MATLAB toolbox for quantum entanglement), and random control qubit drawn from the Hilbert-Schmidt measure (ŻYCZKOWSKI et al., 2011) with a function called *RandomStateVector*, are shown in Figures 4, 5, and 6. Each dot in these plots represents a final density

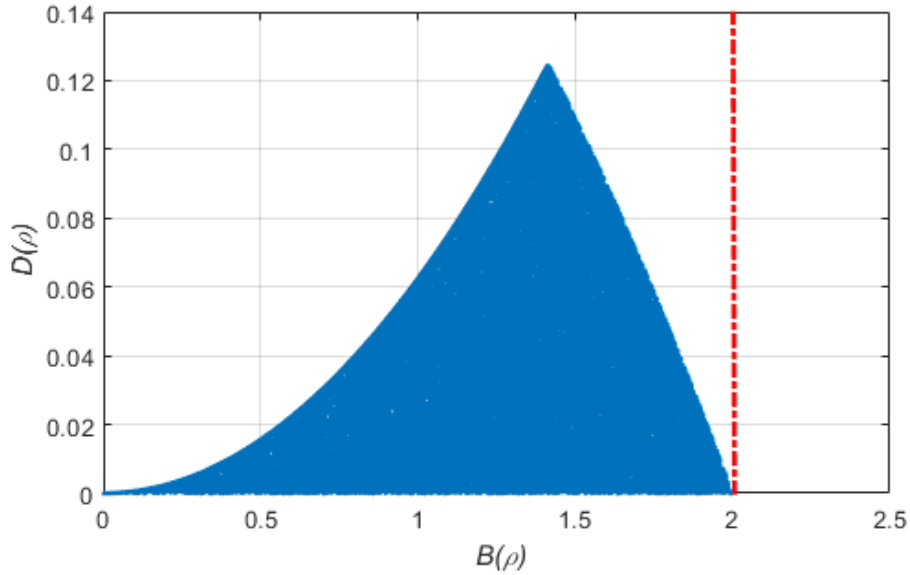

Figure 5 – $D(\rho)$ versus $B(\rho)$ for the DQC1 model with two qubits. Each dot represents the value of these correlations calculated for 10^6 random states. The red dotted line represents the limit value of $B(\rho)$ in which there is no Bell's nonlocality.

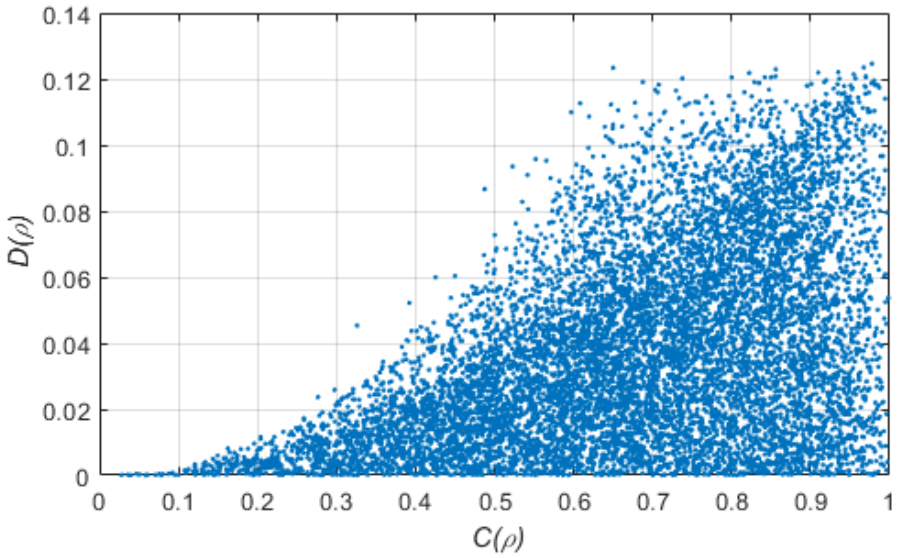

Figure 6 – $D(\rho)$ versus $C(\rho)$ for the DQC1 model with two qubits. Each dot represents the value of these correlations calculated for 10^6 random states.

matrix after running the DQC1 circuit. The maximum value achieved for coherence calculate by eq. 16 is 1, due to control qubit. The red dotted line represents the maximum value for eq. 12 when the density matrix do not show non-local aspects. Notice that this two-qubit model has only coherence and quantum discord (calculated by eq. 15). Since for achieving violation of Bell's inequality is necessary entanglement, Figure 4 shows that we have access to states with Coherence $C(\rho) \neq 0$ but without Bell-violation. Figure

5 shows that this model with two qubits accesses states with $D(\rho) \neq 0$ while there is not violation of Bell's inequality. The quantum discord increases "quadraticaly" as $B(\rho)$ increases until the maximum value 0.1244, then decreases almost linearly. Figure 6 shows that there are many states with small valves of $D(\rho)$ but they present coherence, the fundamental ingredient for existing quantum discord. The number of states in this plot can be distorted because we used different norms, trace norm for coherence and Hilbert-Schmidt norm for quantum discord. As quantum discord is a broader type of correlation than entanglement, it has recently been proposed a quantitative connection between quantum discord and coherence (FERRARO et al., 2010).
The maximum values for the correlations are shown in Table 2. As noticed below, the

Quantum Correlations	Maximum value for Hilbert space	Maximum value for DQC1 model
$B(\rho)$	$2\sqrt{2}$	1.9974
$D(\rho)$	0.5	0.1244
$N(\rho)$	0.5	0
$C(\rho)$	3.0	0.9992

Table 2 – The maximum values of QC between two qubits for the entire Hilbert space and DQC1 model.

DQC1 model of quantum computing is unable to generate strong correlations, as the violation of Bell's inequality, between the control and the auxiliary qubits. At follows we introduce a way to create more powerful correlations to be achieved in DQC1 model.

4.2 DQC1 WITH POST-SELECTION

Here, the goal is to promote the other QC, such as entanglement and Bell-violation in the DQC1 model with two qubits. We base ourselves in (PARKER; PLENIO, 2000) to add the post-selection in this model, in which the authors realize the Shor Factorization algorithm. To promote other correlations in this computation model, we introduced a specific post-selection process after the circuit, which one acts through a filter, described by (KENT; LINDEN; MASSAR, 1999)

$$F = U_a \begin{bmatrix} 1 & 0 \\ 0 & \eta \end{bmatrix} U_a^{\dagger}, \tag{20}$$

with $\eta \in [0,1]$ and U_a is a random unitary operation. This η represents the probability of success of acting this filter.The post-selection with this specific filter makes us trace out a part of the final density matrix. It is allowed erring $1-\eta$, so for $\eta = 1$ it is the same as applying an identity gate on the circuit. Then the circuit operates to purify the auxiliary qubit in the state $\frac{I}{2}$ with a certain η. The circuit with two qubits and the post-selection is

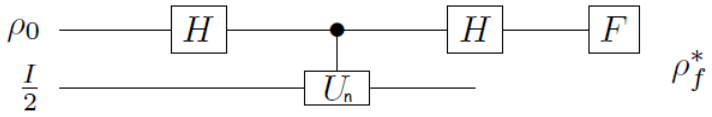

Figure 7 – DQC1 model for two qubits (control ρ_o and auxiliary $\rho_{n=1} = \frac{I}{2}$) with post-selection through a specific filter F that operates in the system. Trace out the control qubit in ρ_f^* we have the auxiliary qubit more purified than before, so that the auxiliary qubit has a degree of purity $P(\rho) > 0.5$. The purification process can be repeated by reinserting the final state of the auxiliary qubit in the circuit again.

shown in Figure 7, where the filter acts like another quantum gate at the circuit. For the study of the promotion of correlations, the control qubit used is a pure random state in the circuit shown in the Figure 3.

Below is the step by step of the circuit

1. A pure random qubit (ρ_0) and the random unitary matrices for the filter and controlled unitary gate are generated through the functions in GETLAB.

2. *Purification process:* an optimization program described by

$$\rho_f^* = arg_\eta min\{P(\rho) : \rho_{final}, F\}$$

runs on the random unitary matrices U_a, where

$$\rho_{final} = (F_0 \otimes I)(H_0 \otimes I)U\left(H_0\rho_0 H_0 \otimes \frac{I}{2}\right)U^\dagger(H_0 \otimes I)(F_0^\dagger \otimes I).$$

Thus, the auxiliary qubit has its final purity $P(\rho_{n=1}) > 0.5$ (purity of $\rho_{n=1} = \frac{I}{2}$).

3. The step 2 was performed m times, thus obtaining a set of N purified

$$\rho_{n=1} = tr_{control}\rho_{final}^*$$

this is the process of finding the purest possible with $P(\rho_{n=1}) = 0.99$ while respecting the cumulative η set at the beginning (see Appendix A).

Figure 8 shows the result of the optimization process made on MATLAB. We found that the chance of totally purifying the auxiliary qubit is zero. That is, the higher the chance of success η of the filter allowed in the purification process, the lower the purity achieved by the control qubit. We will show in section 4.2.2 the plots of QC ($N_N(\rho)$, $D_N(\rho)$, $C_N(\rho)$, $B_N(\rho)$) versus $P(\rho)$. We see the reason for using the purity in the optimization process, because the QC increase with the increase of $P(\rho)$ of the auxiliary qubit.

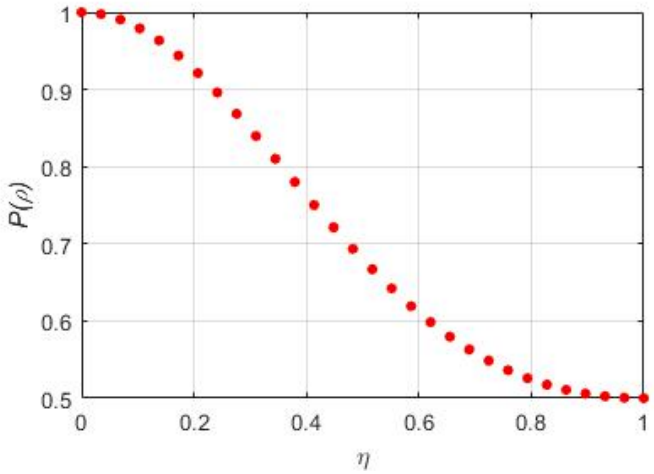

Figure 8 – Purity versus probability of success of the purification process η.

4.2.1 The role of η

In order to investigate the role played by η on the purification process we fixed η and analyzed the minimum value of the purity to entangle and violate the Bell's inequality. Here we evaluate how QC develops along the auxiliary qubit purification process by applying a specific filter, it has the task of purifying the auxiliary qubit. We can describe this process by the black box that purify the auxiliary qubit (see Figure 9). We set a

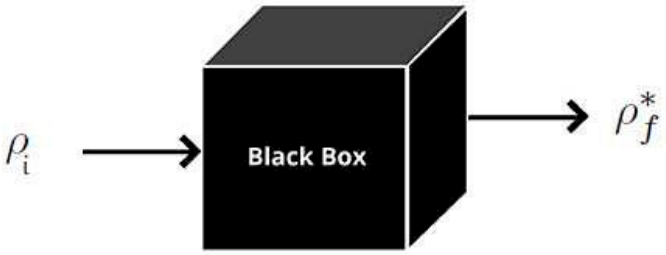

Figure 9 – Optimization process through the black box that purifies the auxiliary qubit.

specific cumulative η as one of these values

$$\frac{1}{2}, \frac{11}{20}, \frac{3}{5}, \frac{13}{20}, \frac{2}{3}, \frac{7}{10}, \frac{3}{4}, \frac{4}{5}, \frac{5}{6}, \frac{9}{10}, \frac{19}{20}, \frac{24}{25}, \frac{49}{50}$$

and we perform the purification steps describes in section 4.2. In order to increase data confidence, we execute $m = 400$ times the circuit (Figure 7) for each η with $N = 10^4$ random unitary matrices $U_{n=1}$ and U_a. Then we have a set of N purified $\rho_{n=1}$ which are used to calculate the N values of the correlations. We choose some values of cumulative η to analyze the behavior of QC. All plots of mean values of QC are normalized to one, where we used for this the maximum value that each correlation can reach (see Table 2). Each point in these plots is an average value of m random states used to calculate

the QC for a purification process of N random states. Due to the optimization process, these plots present a finite sample of states, and presents surfaces with smaller widths, making it evident that the optimization process retains states that have low performance in both correlations. With the increase in the purity of the control qubit we have access to states with more QC.

Figure 10 shows the relation between the $B(\rho)$ and quantum discord, the red dotted line limits the maximum value that $B(\rho)$ can reach without violation. We note that with the decrease of η the value of $B(\rho)$ comes closer to the maximum Bell-violation, i.e., the value of this QC increases, for η smaller we have more Bell-violation. We already expected this behavior because of Figure 5, that without applying the filter we did not reach Bell-violation. We also observe that the $B(\rho)$ always starts from a nonzero value. As well, we note the relation with Figure 8, that for $\eta \sim 1$ is same that do not apply any filter in the circuit and the auxiliary qubit keeps your initial purity. Figures 10 (*a*) and 10 (*b*) contain few states with Bell-violation and non-null quantum discord, while Figure 10 (*c*) shows that we can have Bell-violation with small $D(\rho)$.

Figure 11 shows the relation between the $B(\rho)$ and negativity. It is observed that with the decrease of η we have access to states that present higher values of entanglement and that reach Bell-violation. The number of states with the null negativity decrease as η decrease as expected for the DQC1 circuit without post-selection, where we do not have entanglement. We can not have Bell-violation without entanglement. As well, we also note the relation with Figure 8, that for $\eta \sim 1$ we do not have states with violation of Bell's inequality or entanglement.

Figure 12 shows the relationship between the $B(\rho)$ and coherence. It is evident that in all plots we do not have states with zero coherence, showing that coherence is not important to achieve Bell-violation. The maximum coherence that the states can achieve is 0.35 for this two qubits computing model. As η increases we approach the behavior of Figure 4, in which all states with only QC of coherence type do not violate Bell's inequality.

Figure 13 shows the relation between coherence and quantum discord. The number of states with null quantum discord increase with the increase of η. As we observed previously, the coherence never reaches zero value. As expected, with the increase of η we approach the result of the Figure 6. The maximum value of quantum discord decrease with the increase of η.

Figure 14 shows the relation between the negativity and coherence. We do not have states with null coherence, showing that coherence is not important to achieve non-null entanglement. As η increases, we have smaller chance of finding states with $N(\rho) > 0$, i.e., the maximum value of negativity that states can achieve decreases with the increase of η, as expect of section 4.2.

Figure 15 shows the relation between the negativity and quantum discord. It is

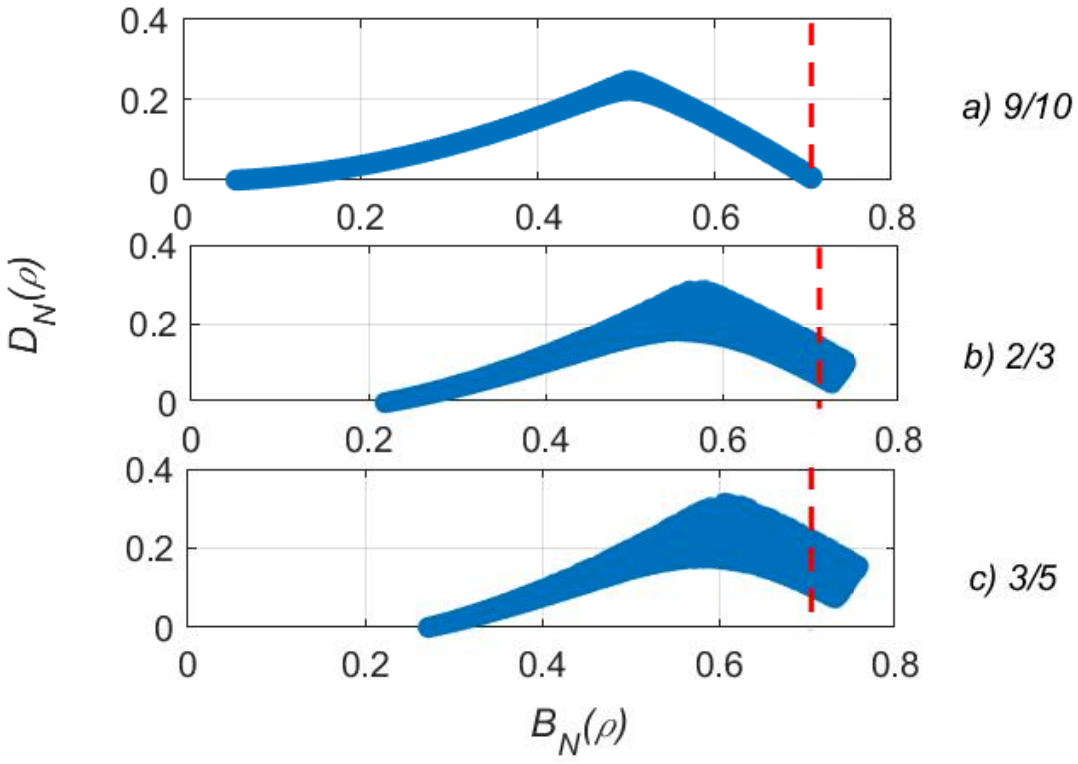

Figure 10 – Plots of the normalized quantum discord $D_N(\rho)$ versus normalized $B_N(\rho)$ for different values of η, (a) $\eta = 9/10$, (b) $\eta = 2/3$, and (c) $\eta = 3/5$. Each point in the sample of $N = 10^4$ points (different final density matrices) were obtained by averaging over $m = 400$ random purification processes in which U_a could vary. The red dotted line indicates the lower bound of the violation of the normalized Bell's inequality $1/\sqrt{2}$.

shown that we have many states with the value of $N_N(\rho) > 0.15$ and a small value of quantum discord. This behavior changes for greater values of η. We can obtain states with null quantum discord and low entanglement. These QC grow linearly until they reach a maximum value 0.24 and from there we have many states with greater values of negativity.

In all plots, we recovered the behavior presented in the DQC1 model without post-selection. As commented in the previous subsection, a consequence of optimize the purity implies that we have access a number of states with others correlations greater than that present in the DQC1 model without post-selection.

The maximum mean values of normalized QC for specific cumulative η are shown in Figures 16, 17, 18, and 19. Analyzing the pattern for $\eta \sim 1$ in these plots, we recover the behavior of all QC without post-selection, as shown in Figures 4, 5, and 6. Figure 16

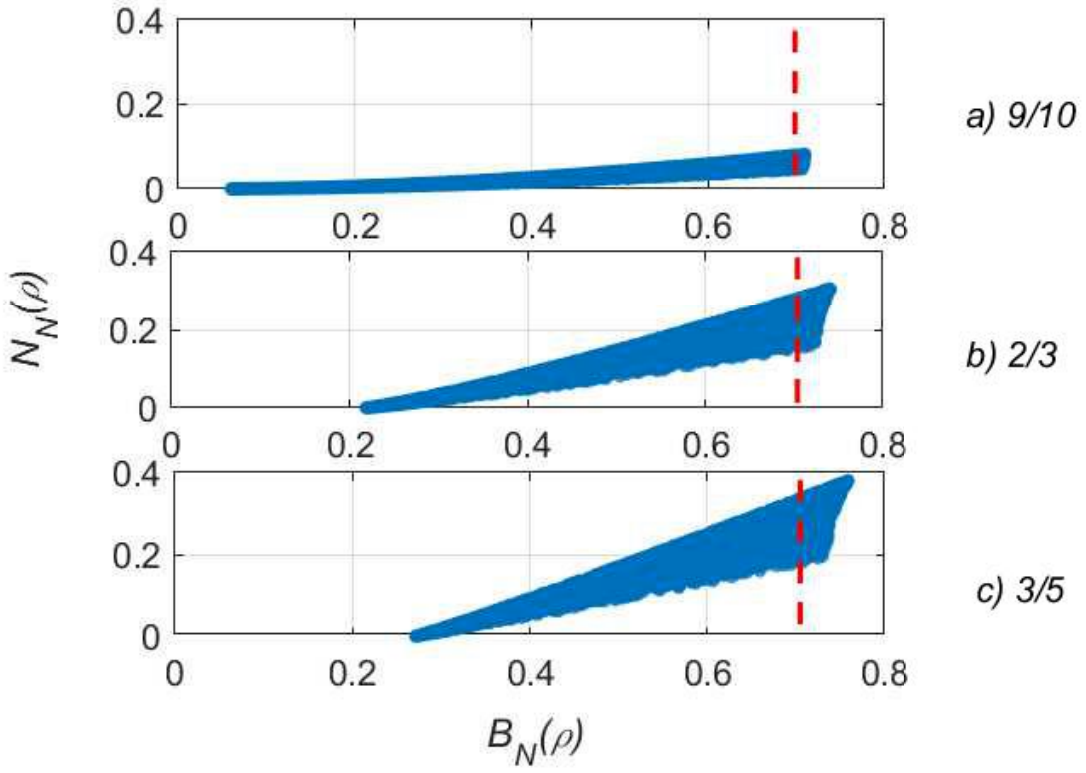

Figure 11 – Plots of the normalized negativity $N_N(\rho)$ versus normalized $B_N(\rho)$ for different values of η, (a) $\eta = 9/10$, (b) $\eta = 2/3$, and (c) $\eta = 3/5$. Each point in the sample of $N = 10^4$ points (different final density matrices) were obtained by averaging over $m = 400$ random purification processes in which U_a could vary. The red dotted line indicates the lower bound of the violation of the normalized Bell's inequality $1/\sqrt{2}$.

shows normalized $B(\rho)$ versus η. As η approaches to one we get the lower Bell-violation value. This means that with an optimization that slightly purifies the auxiliary qubit, we already achieve the violation of Bell's inequality. Figure 17 shows normalized $C(\rho)$ as a function of the purification parameter η. The coherence reaches its maximum value of ~ 0.35. Figure 18 shows normalized $D(\rho)$ as a function of the purification parameter η. The minimum of quantum discord reached is near to $D(\rho) \sim 0.24$. Even for $\eta \sim 1$ the quantum discord does not achieve zero. Figure 19 shows normalized $N(\rho)$ as a function of the purification parameter η. The value of negativity decreases linearly with the increasing of η until it reaches the null value.

According to the analysis of this section, we can conclude that even a filter with $\eta < 1$ is sufficient to promote QC in DQC1 model with two qubits, so that the entanglement and violation of Bell's inequality arise in this system

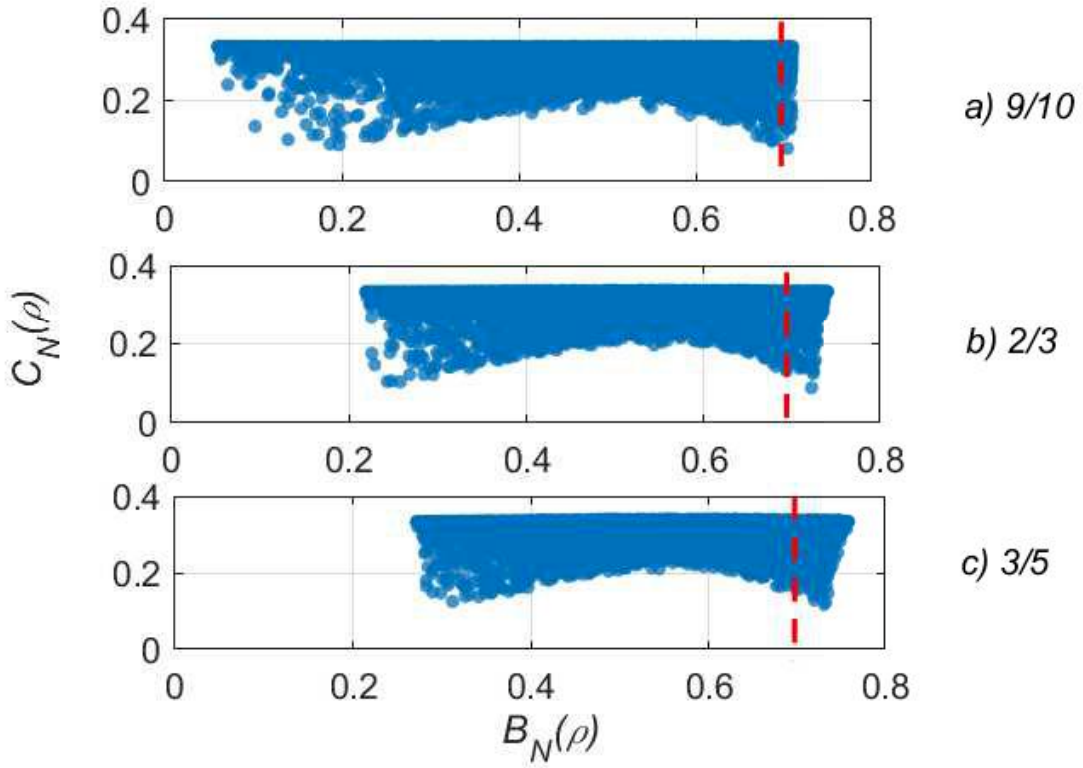

Figure 12 – Plots of the normalized coherence $C_N(\rho)$ versus normalized $B_N(\rho)$ for different values of η, (a) $\eta = 9/10$, (b) $\eta = 2/3$, and (c) $\eta = 3/5$. Each point in the sample of $N = 10^4$ points (different final density matrices) were obtained by averaging over $m = 400$ random purification processes in which U_a could vary. The red dotted line indicates the lower bound of the violation of the normalized Bell's inequality $1/\sqrt{2}$.

4.2.2 The purity of the auxiliary qubit

In this section we will explore the role of purity of the auxiliary qubit in DQC1 model with two qubits. What is the minimum purity necessary for entanglement-like correlation to appear in this system. We observe that even without a significant purification of the auxiliary qubit we already achieve non-null entanglement and Bell-violation. Figure 20 shows the relation between purity and the filter parameter η, it is a complement for Figure 8. We observe that the maximum mean value of the purity is $P(\rho) = 0.6167$.

Figures 21, 22, 23, and 24 show the behavior each normalized quantum correlation as function of the purity of the auxiliary qubit. We note that the maximum mean value of the purity achieve is 0.62. Figure 21 shows that even with the auxiliary qubit in the maximally mixed state, we already have a nonzero coherence value and as the purity of the auxiliary qubit increases, the coherence also increases approximately linearly.

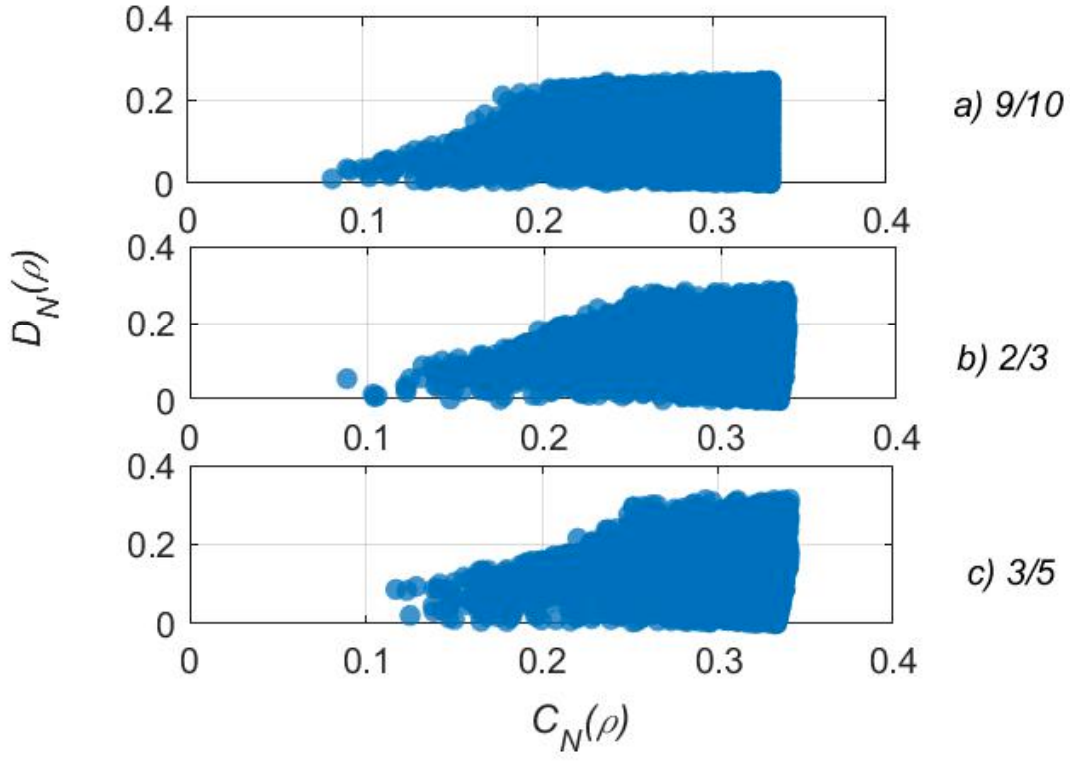

Figure 13 – Plots of the normalized quantum discord $D_N(\rho)$ versus normalized coherence $C_N(\rho)$ for different values of η, (a) $\eta = 9/10$, (b) $\eta = 2/3$, and (c) $\eta = 3/5$. Each point in the sample of $N = 10^4$ points (different final density matrices) were obtained by averaging over $m = 400$ random purification processes in which U_a vary.

Figure 22 shows that negativity increases with the increase of purity, starting from zero negativity until reaching a maximum of 0.5 for a purity of the control qubit of $P(\rho) \sim 0.62$. Figure 23 shows that quantum discord starts from a non-null value and not increase so much with the increase of purity. Figure 24 shows that the $B(\rho)$ increases with the purity, however, without reaching the maximum violation. Also with a small purification of auxiliary qubit, we already achieve the Bell-violation.

The behavior of the plots shows that we need little purification of the control qubit in order to have non-null entanglement and violation of Bell's inequality. In this way, we can execute the optimization program to purify the auxiliary qubit just a few steps and have entanglement and violation of Bell's inequality. Figure 25 shows the relation between normalized QC, η, and purity of the auxiliary qubit. It is a summary of the last two subsections.

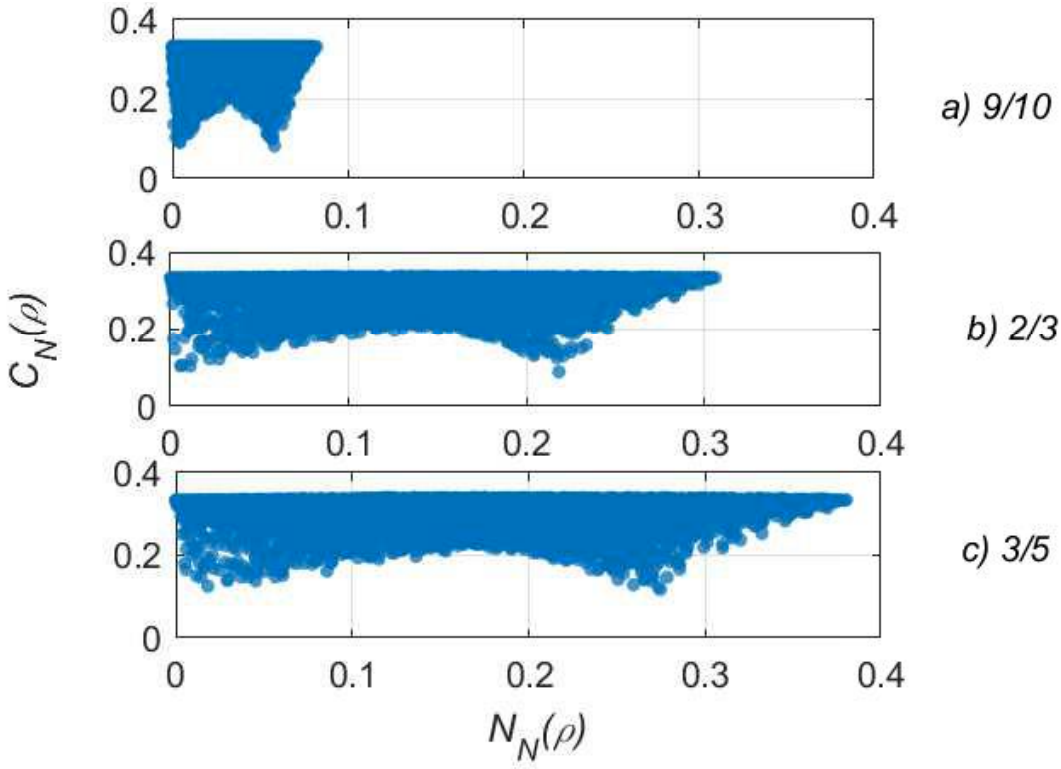

Figure 14 – Plots of the normalized coherence $C_N(\rho)$ versus normalized negativity $N_N(\rho)$ for different values of η, (a) $\eta = 9/10$, (b) $\eta = 2/3$, and (c) $\eta = 3/5$. Each point in the sample of $N = 10^4$ points (different final density matrices) were obtained by averaging over $m = 400$ random purification processes in which U_a vary.

4.2.3 Purification optimization

We can analyze the QC for different purities of the auxiliary qubit without set the cumulative η. Thus, it is also a parameter for optimizing in MATLAB until reaching $P(\rho) = 0.99$. We execute the program many times and it was necessary on average 12 interactions with the optimization program to achieve the maximum value of purity. In other words, on average, twelve applied differents filters in DQC1 circuit with two-qubit were required to reach the maximum purity.

The relation between the QC with steps of purification are shown in Figure 26, 27, 28, 29, 30, and 31. Each surface with different color shows the mean value of 10^4 random unitary matrices used to compute the QC for each purification step of the auxiliary qubit. The intermediate steps are similar, and for this reason, we have plotted only 5 of 12 steps, i.e., the first, second, third, fourth, and twelfth ones. The blue surface represents the mean value of QC after the first step of purification, while the green one after the

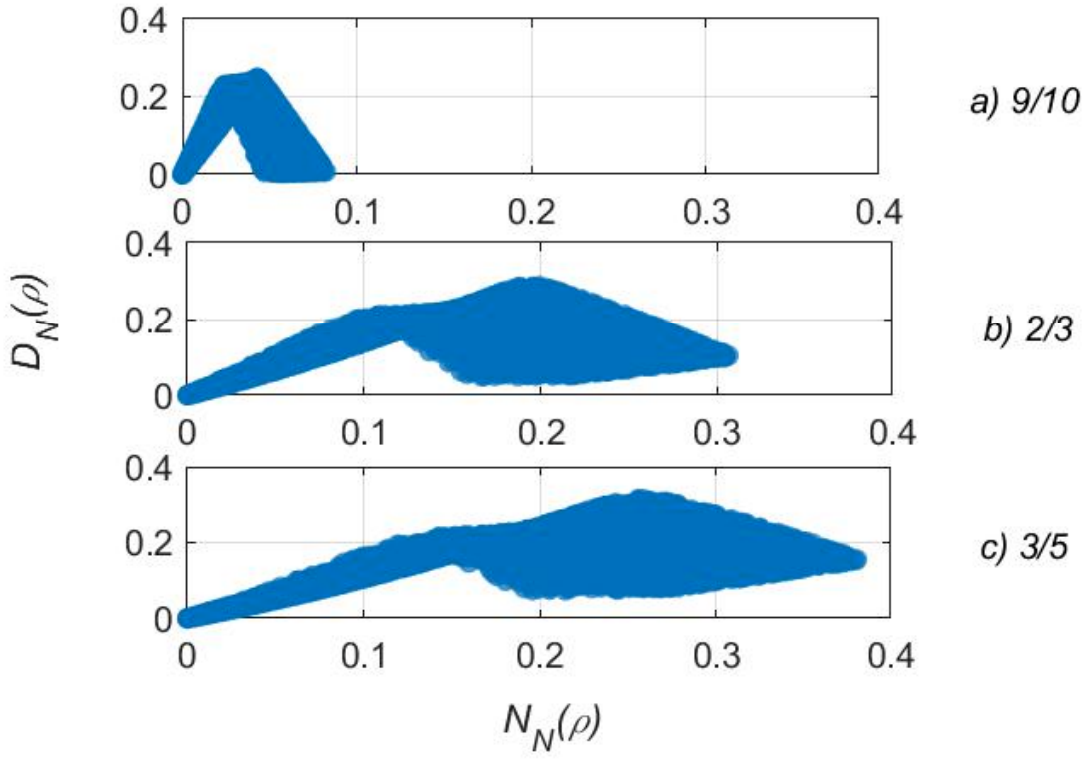

Figure 15 – Plots of the normalized quantum discord $D_N(\rho)$ versus normalized negativity $N_N(\rho)$ for different values of η, (a) $\eta = 9/10$, (b) $\eta = 2/3$, and (c) $\eta = 3/5$. Each point in the sample of $N = 10^4$ points (different final density matrices) were obtained by averaging over $m = 400$ random purification processes in which U_a vary.

last step of purification, in which the auxiliary qubit achieves $P(\rho)$ 0.99.

Figure 26 shows that according to the increase of the purity of the auxiliary qubit, the number of states that violates the Bell's inequality also increases near the maximum violation, while states with greater discord also increase. For the purity of 0.99, practically all states violate the Bell's inequality. Figure 27 shows that we need more steps of purification to reach states with maximum negativity. We note that little entanglement is possible to violate Bell's inequality. Figure 28 shows that in all steps of purification of the auxiliary qubit, the states have non-null coherence, until achieving the maximum value of 1.5. Figure 29 shows that we can have states with null discord and non-null coherence. For the last step of purification, almost all states have $C(\rho) > 1$. Figure 30 shows that for the maximum purification, all states have $C(\rho) > 1$ and almost states with $N(\rho) > 0.15$. Also, we can have coherence even without entanglement, as expect from section 4.1. Figure 31 shows that with the increase of purity of the auxiliary qubit, we

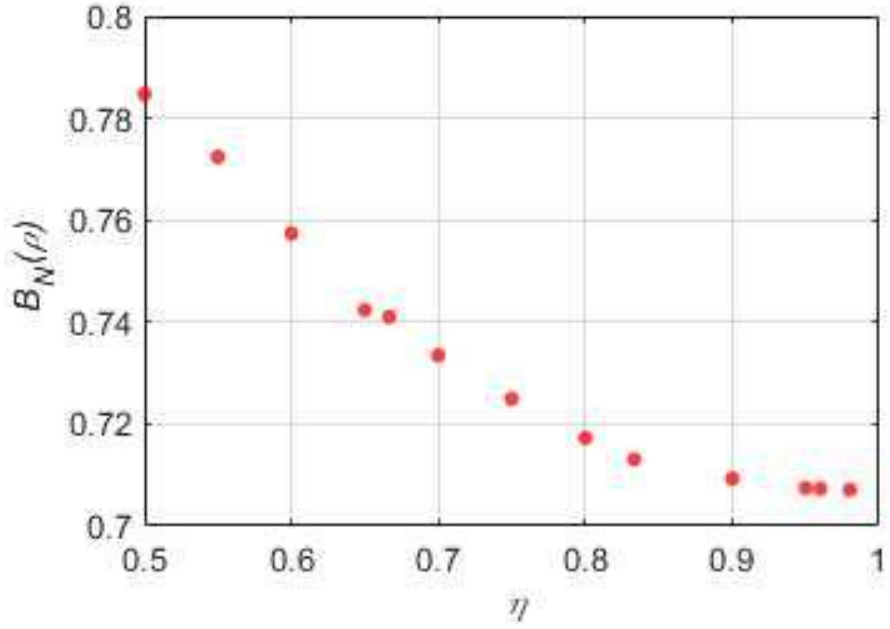

Figure 16 – Normalized $B_N(\rho)$ versus η. Each dot represents the maximum value for this correlation with a specific η.

have access to more states with the non-null negativity and non-null quantum discord.

We can note that upon reaching the maximum purity (0.99) the correlations also reach their maximum accessible values. The $B(\rho)$ almost achieves the maximum value of $2\sqrt{2}$ for the most purified auxiliary qubit. Negativity also reaches its maximum value 0.5. Comparing with Figures 10, 11, 12, 13, 14, and 15 of the subsection 4.2.1, we can notice the same pattern for a determined purity. We achieve states with more QC, as entanglement and Bell's nonlocality, than previously without the post-selection .

4.2.4 Density of states with quantum correlations in DQC1 circuit with post-selection

Density of states is defined as the ratio between the number of states with a correlation value greater than that achieved by the states in the DQC1 model with two qubits without post-selection (see Table 2) and the amount of total states (10^4). Figures 32, 33, and 34 present density of states of between coherence, quantum discord, and Bell's nonlocality for the different values of η. The values of η are the same used before in subsection 4.2.1. From plots for different η in subsection 4.2.1 we can infer that we have few states that violate the Bell's inequality if compared to other QC. We observe that the higher the η the lower the density of states that overcome the value of these correlations for DQC1 model without post-selection. This result recovers the behavior shown in Figures 4, 5, and 6. Figure 32 shows the relation between the density of states with quantum discord greater 0.1244 for some values of the filter parameter η. We can

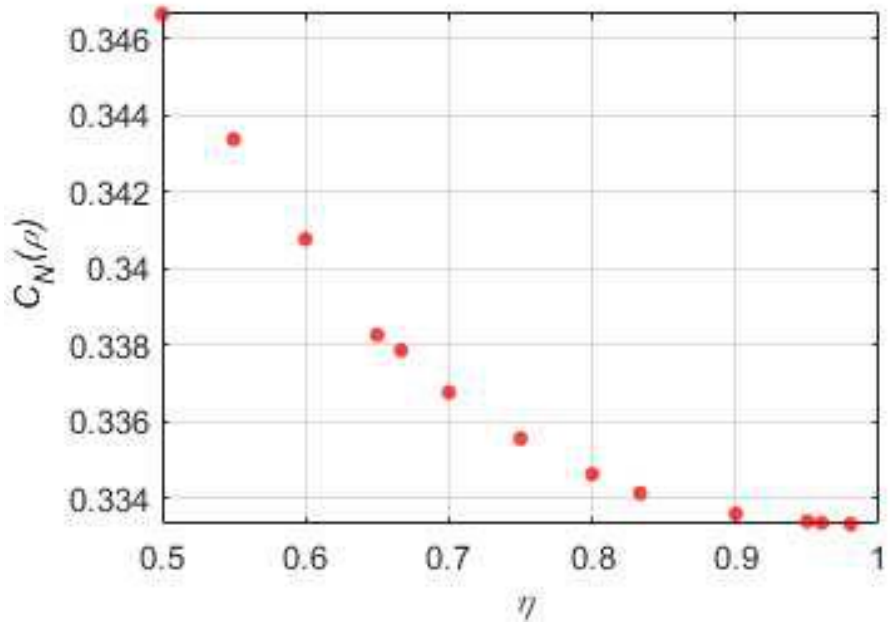

Figure 17 – Normalized coherence $C_N(\rho)$ versus η. Each dot represents the maximum value for this correlation with a specific η.

observe that the density of states are greater for small η. Figure 33 shows the relation between the density of states with coherence greater than 0.9992 for some values of the filter parameter η. And Figure 34 shows the relation between the density of states with Bell's quantifier greater than 1.9974 for some values of the filter parameter η. As in other plots we can also observe that the density of states are greater for small η. These plots complement the information obtained with the previous plots for $\eta \sim 1$ that recovered the results of the correlations for the DQC1 model with two qubits.

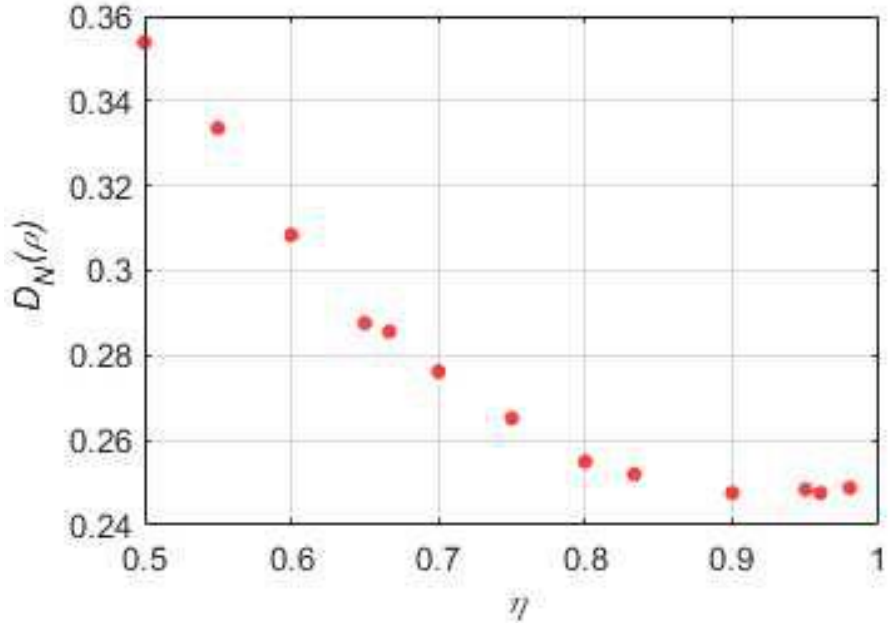

Figure 18 – Normalized quantum discord $D_N(\rho)$ versus η. Each dot represents the maximum value for this correlation with a specific η.

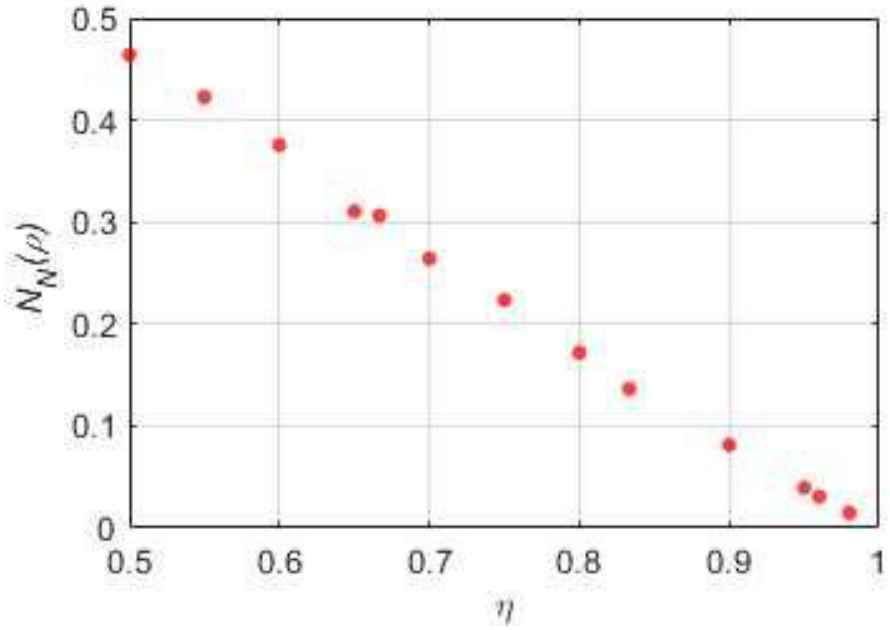

Figure 19 – Normalized negativity $N_N(\rho)$ versus η. Each dot represents the maximum value for this correlation with a specific η.

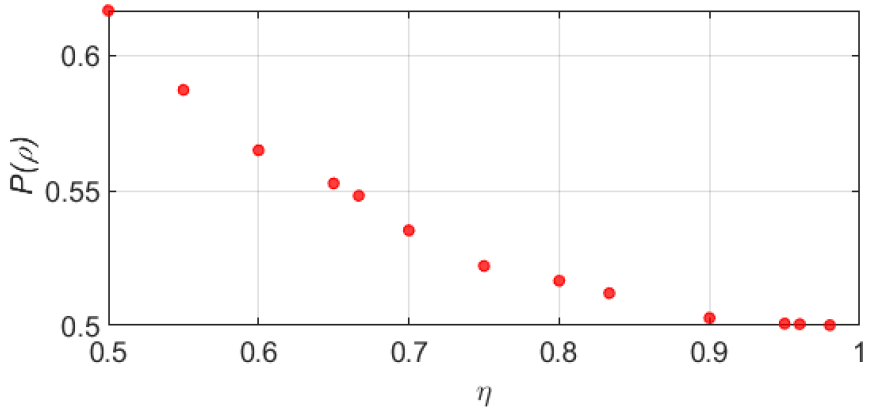

Figure 20 – Purity as function of the probability of success η for DQC1 model with two qubits with the post-selection. Each dot represents the maximum mean value of the achieved purity for the auxiliary qubit with a specific η.

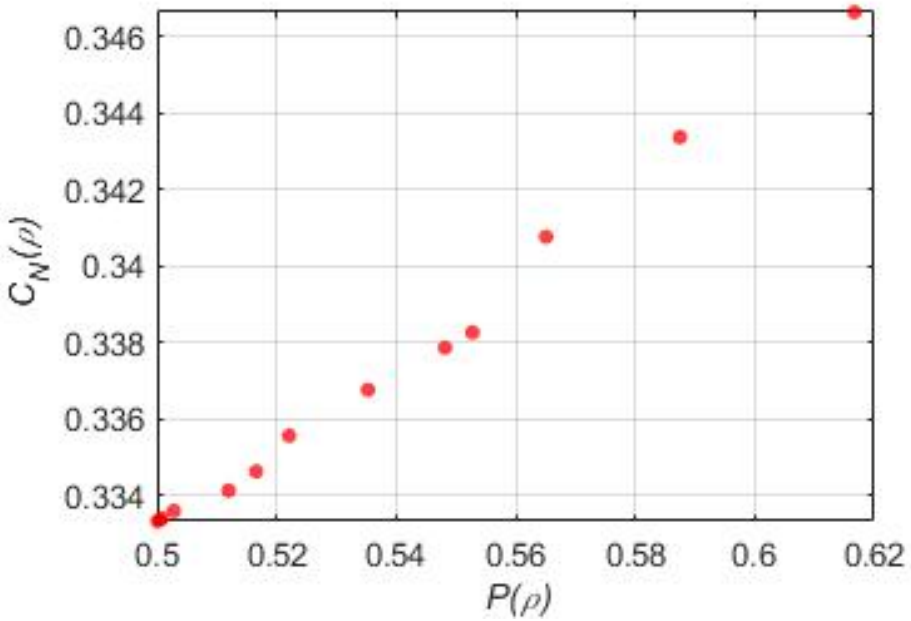

Figure 21 – Normalized coherence $C_N(\rho)$ versus $P(\rho)$. Each dot represents the maximum mean value for this correlation with a specific purity.

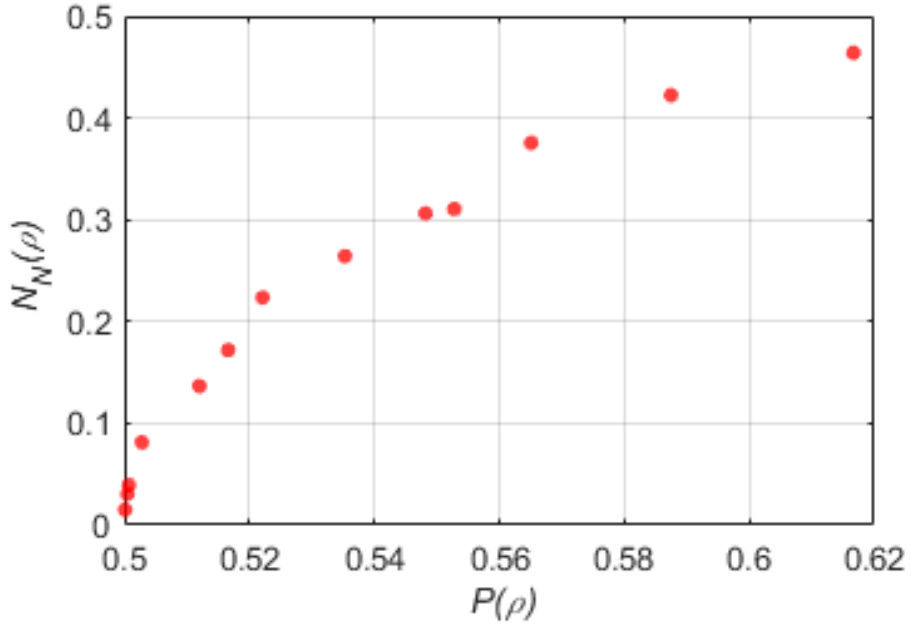

Figure 22 – Normalized negativity $N_N(\rho)$ versus $P(\rho)$. Each dot represents the maximum mean value for this correlation with a specific purity.

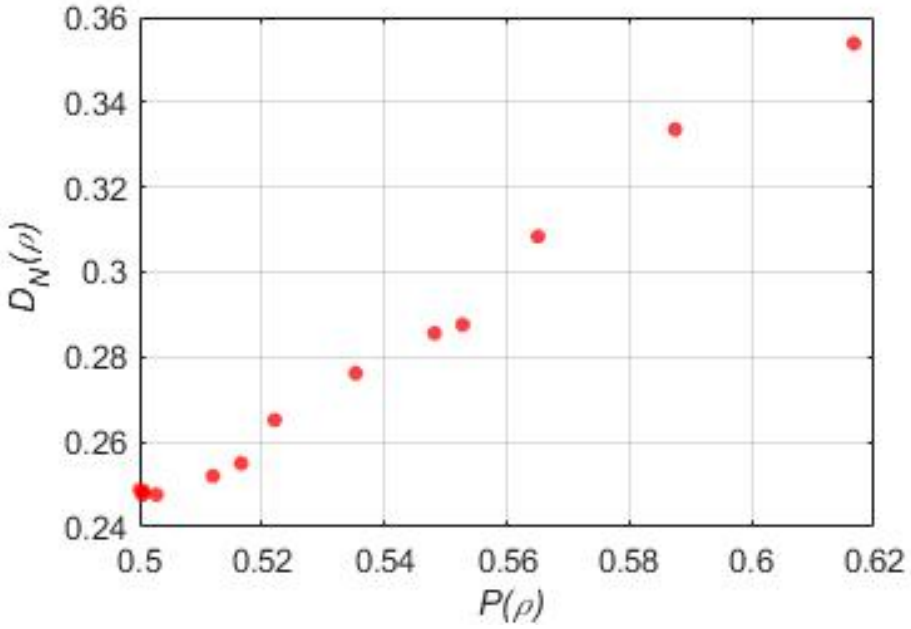

Figure 23 – Normalized quantum discord $D_N(\rho)$ calculate from eq. 15 as function of the purity $P(\rho)$. Each dot represents the maximum mean value for this correlation with a specific purity.

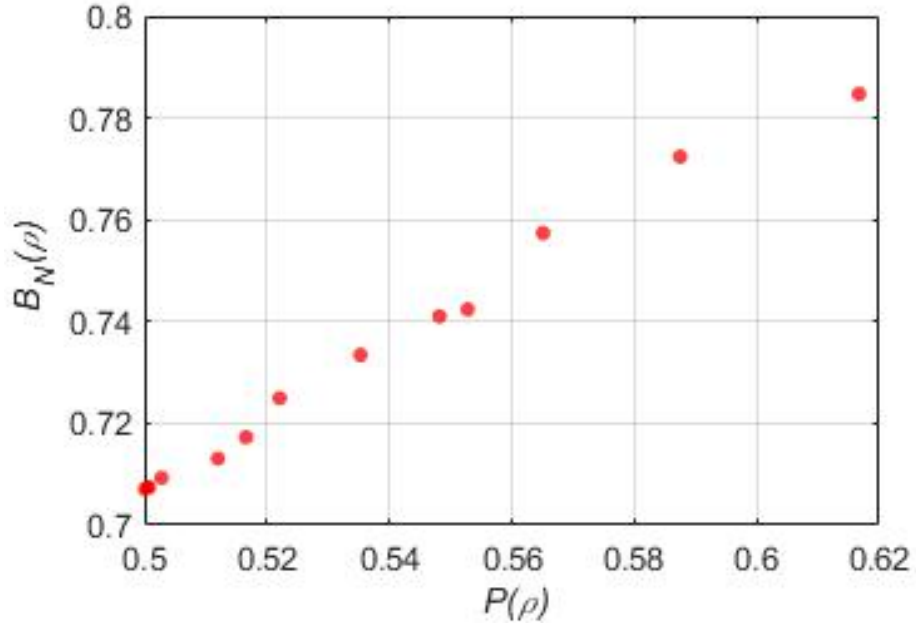

Figure 24 – Normalized $B_N(\rho)$ versus $P(\rho)$. Each dot represents the maximum mean value for this correlation with a specific purity.

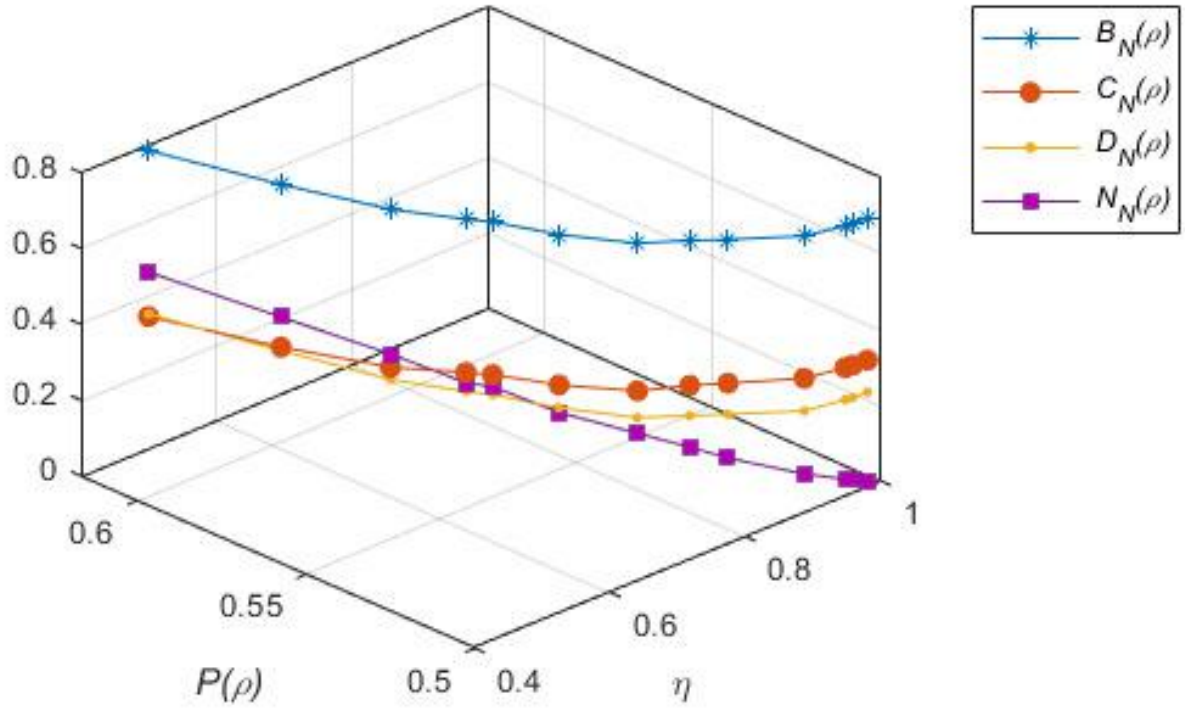

Figure 25 – Relation between η, the maximum mean value of purity and the normalized QC for the DQC1 model with post-selection.

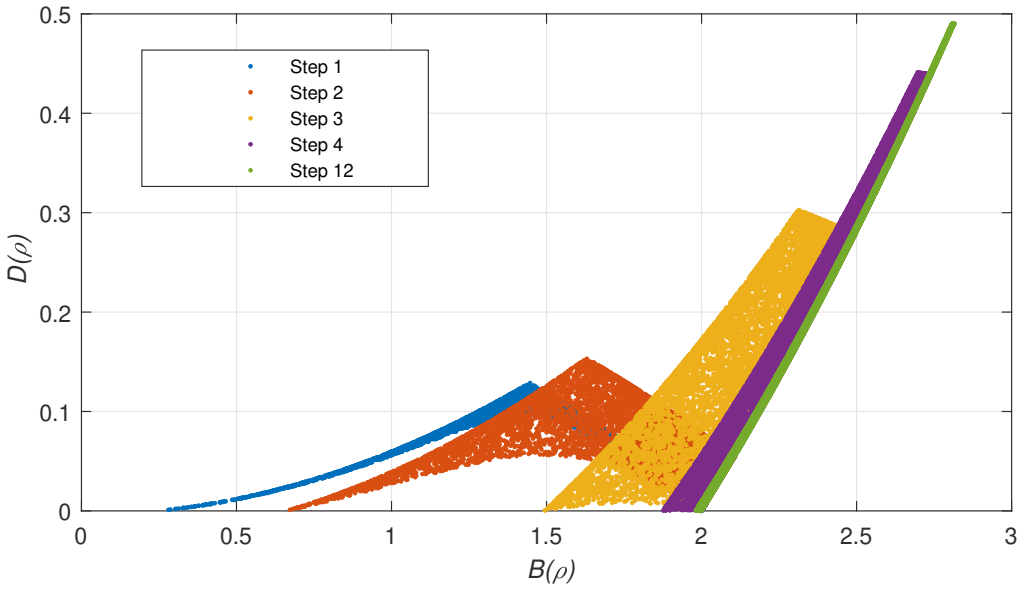

Figure 26 – $D(\rho)$ versus $B(\rho)$. Each surface with different color shows the mean value of 10^4 random unitary matrices used to compute the QC for each purification step of the auxiliary qubit. As the behavior of the quantum correlations is similar for the intermediate steps of the purification, such surfaces have not been plotted.

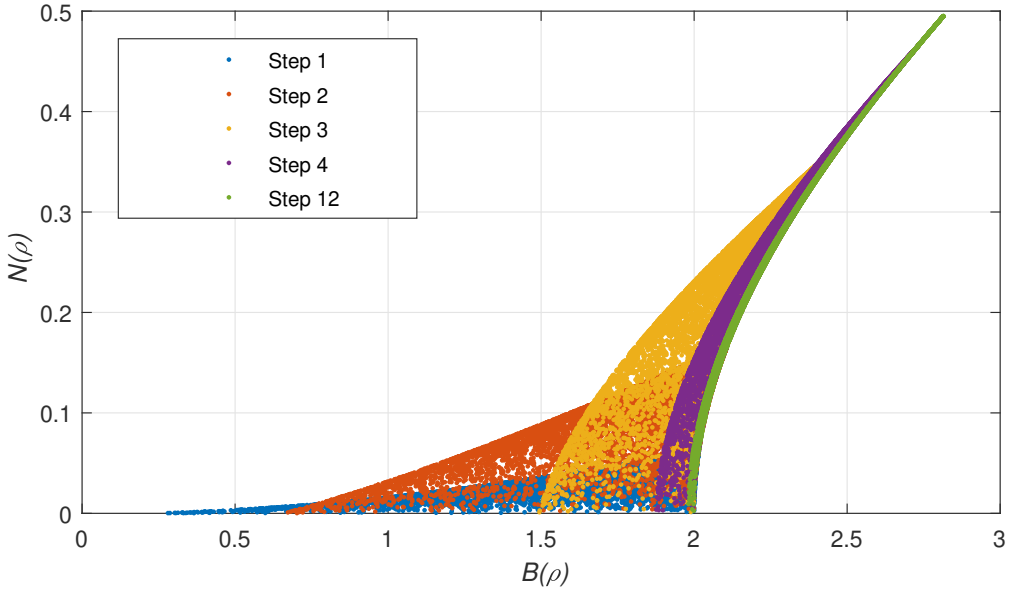

Figure 27 – $N(\rho)$ versus $B(\rho)$. Each surface with different color shows the mean value of 10^4 random unitary matrices used to compute the QC for each purification step of the auxiliary qubit. As the behavior of the quantum correlations is similar for the intermediate steps of the purification, such surfaces have not been plotted.

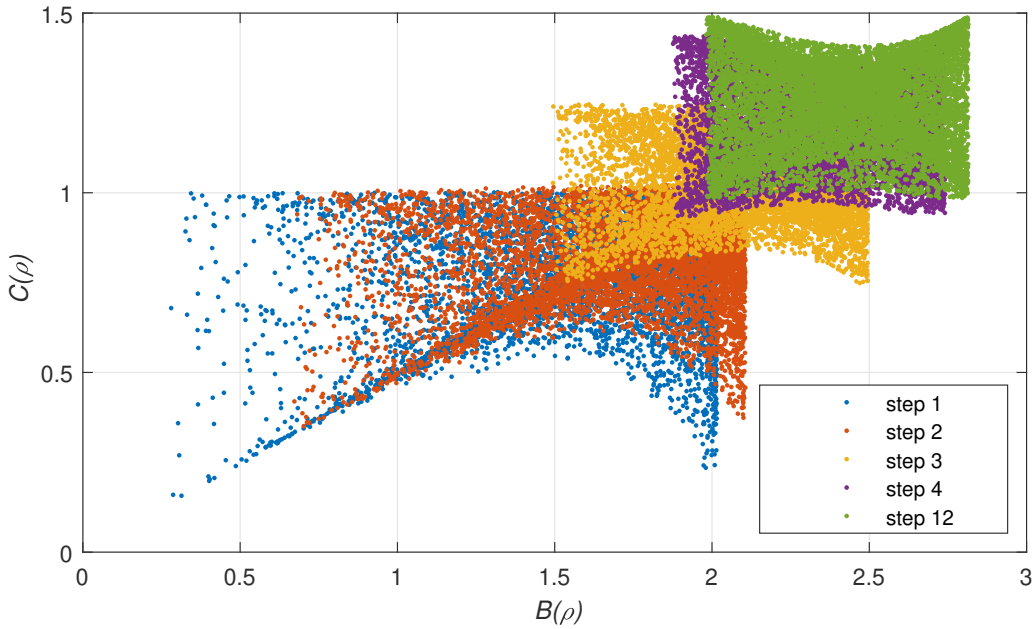

Figure 28 – $C(\rho)$ versus $B(\rho)$. Each surface with different color shows the mean value of 10^4 random unitary matrices used to compute the QC for each purification step of the auxiliary qubit. As the behavior of the quantum correlations is similar for the intermediate steps of the purification, such surfaces have not been plotted.

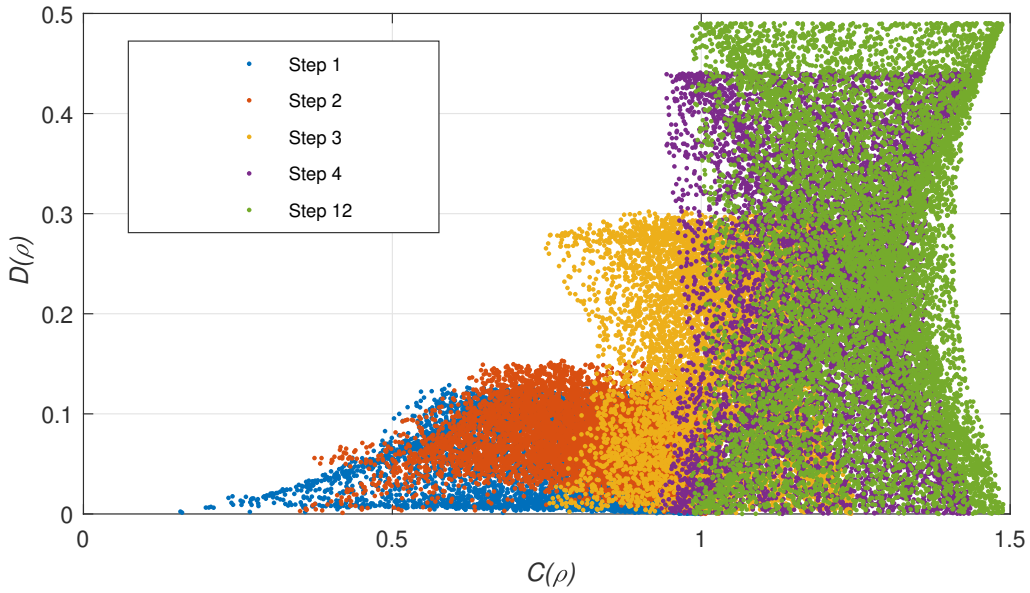

Figure 29 – $D(\rho)$ versus $C(\rho)$.Each surface with different color shows the mean value of 10^4 random unitary matrices used to compute the QC for each purification step of the auxiliary qubit. As the behavior of the quantum correlations is similar for the intermediate steps of the purification, such surfaces have not been plotted.

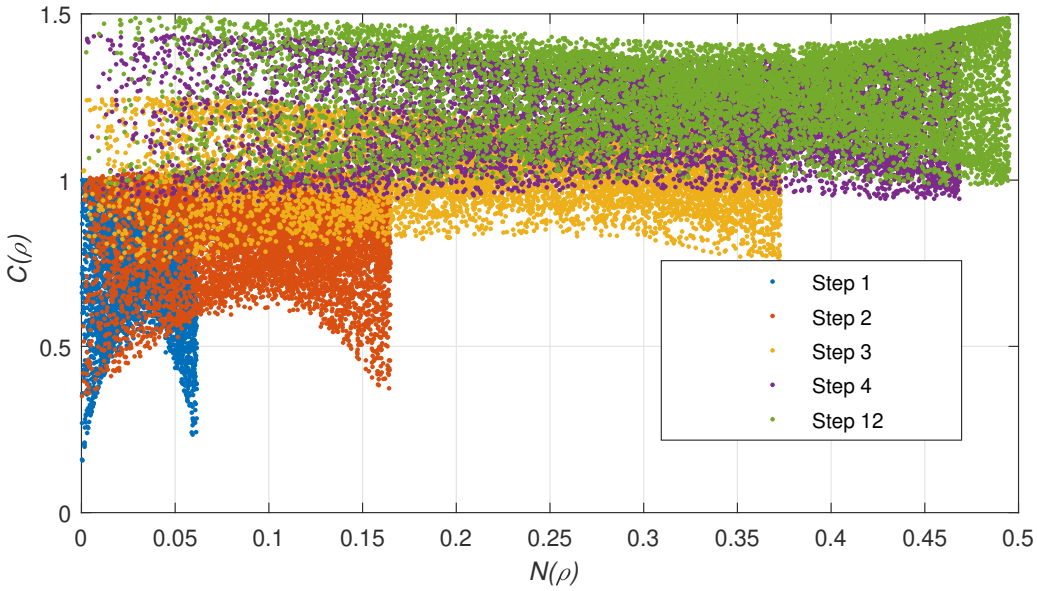

Figure 30 – $C(\rho)$ versus $N(\rho)$. Each surface with different color shows the mean value of 10^4 random unitary matrices used to compute the QC for each purification step of the auxiliary qubit. As the behavior of the quantum correlations is similar for the intermediate steps of the purification, such surfaces have not been plotted.

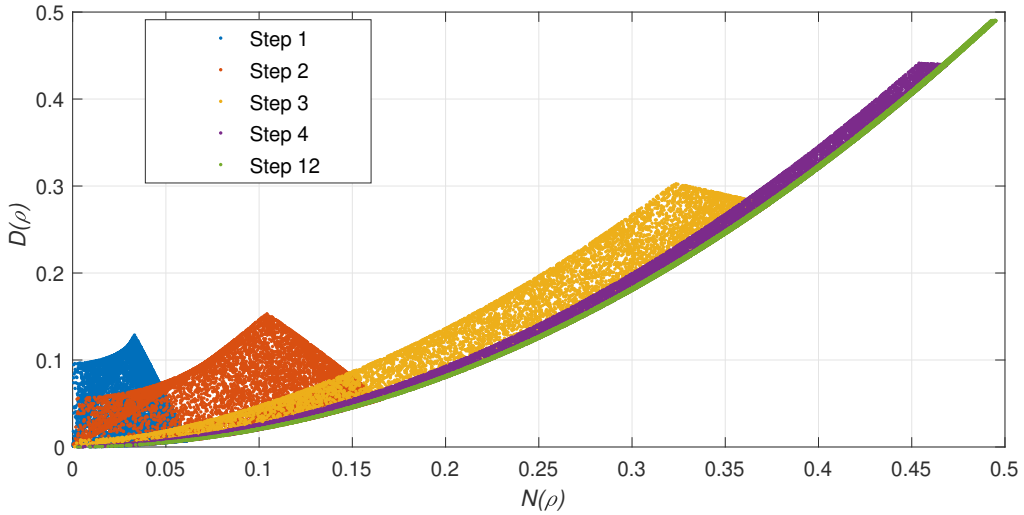

Figure 31 – $D(\rho)$ versus $N(\rho)$. Each surface with different color shows the mean value of 10^4 random unitary matrices used to compute the QC for each purification step of the auxiliary qubit. As the behavior of the quantum correlations is similar for the intermediate steps of the purification, such surfaces have not been plotted.

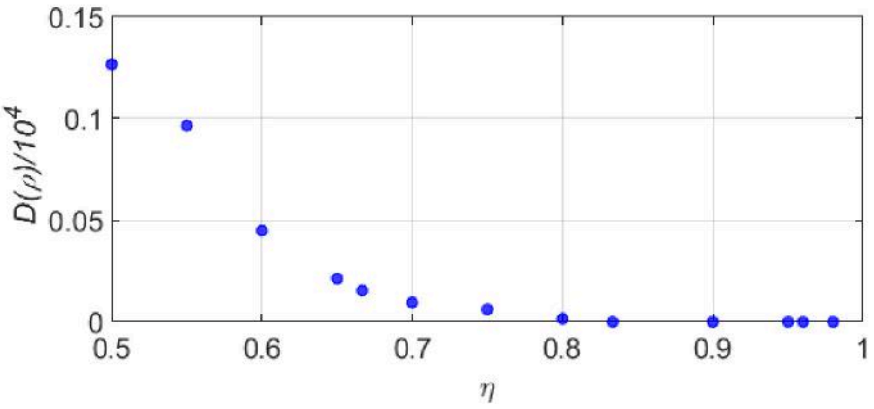

Figure 32 – Density of states with values of quantum discord above the values achieved by the states in the usual DQC1 model, i.e., without post-selection, versus the probability of success η of the purification protocol. The total number of states is 10^4.

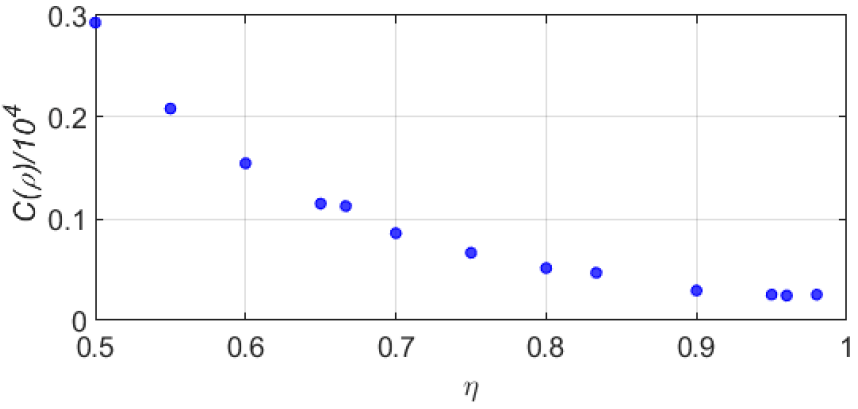

Figure 33 – Density of states with values of coherence above the values achieved by the states in the usual DQC1 model, i.e., without post-selection, versus the probability of success η of the purification protocol. The total number of states is 10^4.

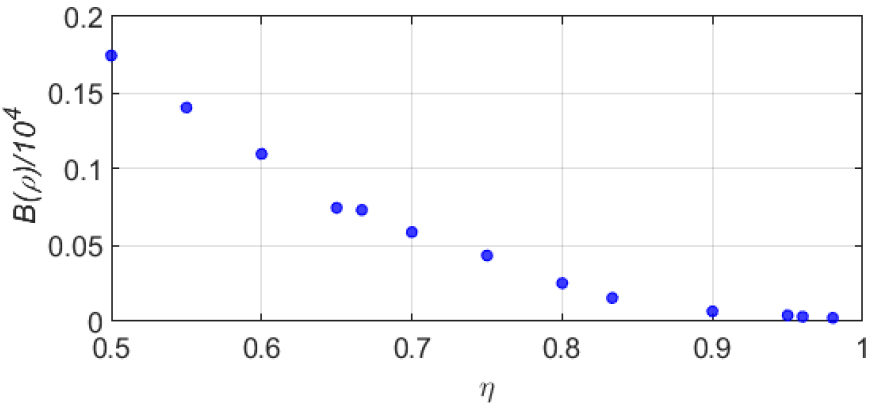

Figure 34 – Density of states with values of $B(\rho)$ above the values achieved by the states in the usual DQC1 model, i.e., without post-selection, versus the probability of success η of the purification protocol. The total number of states is 10^4.

5 CONCLUSION

In this work, quantum correlations in the DQC1 model with two qubits were studied. As described in the literature, this model has no entanglement, thus, this resource is not responsible for the advantage over classical computing for the evaluation of the normalized trace of unitary operations. As this model with two qubits does not have entanglement, neither Bell-violation, because we cannot have a violation of Bell inequality without entanglement between qubits. To find the other QC not previously present in this model with two qubits, a post-selection with a specific filter with a parameter η was added into the circuit. This allowed us to perform an auxiliary qubit purification process through optimization programs of the purity, the random unitary matrices of the filter, and controlled unitary gate. Setting the maximum purity achieved in this optimization process to 0.99, we realize that the filter parameter must be close to 1, that which is the same as applying an identity gate. For specific cumulative η we recalculate the plots of QC for the DQC1 model with two qubits, and we detect that the lower the η, the higher the correlation values will be achieved. We also analyze the role of purity of the auxiliary qubit in relation to the QC and we found that for a small purity entanglement and Bell violation already begin to appear. To be more precise, we need a purity of 0.62 to have these correlations. A study of the average number of purification steps that are needed to achieve maximum purity of 0.99 was also done, on average 12 purification steps are required and we find the maximum Bell-violation and maximum entanglement for the maximally pure auxiliary qubit.

It was demonstrated in (PARKER; PLENIO, 2000) that a single pure qubit, together with an initial supply of $log_2 N$ qubits in an arbitrarily mixed state with the post-selection, is sufficient to implement Shor's algorithm for the factorization of the number N efficiently. Our result goes in the direction that in order to use the DQC1 model to solve the factoring problem as done by (PARKER; PLENIO, 2000), the purification process was necessary because just as we show several correlations are generated in the system.

We can further expand our studies, executing the program for a larger number of random unitary matrices and for a greater number of auxiliary qubits in order to verify whether this behavior is maintained for the access to others quantum correlations.

REFERÊNCIAS

ABERG, Johan. Quantifying superposition. **arXiv preprint quant-ph/0612146**, 2006.

ADESSO, Gerardo; BROMLEY, Thomas R; CIANCIARUSO, Marco. Measures and applications of quantum correlations. **Journal of Physics A: Mathematical and Theoretical**, IOP Publishing, v. 49, n. 47, p. 473001, 2016.

ARRUDA, Luiz Gustavo Esmenard. **Computação quântica baseada em medidas projetivas em sistemas quânticos abertos**. 2011. PhD thesis – Universidade de São Paulo.

ASPECT, Alain; GRANGIER, Philippe; ROGER, Gérard. Experimental realization of Einstein-Podolsky-Rosen-Bohm Gedankenexperiment: a new violation of Bell's inequalities. **Physical review letters**, APS, v. 49, n. 2, p. 91, 1982.

BALLENTINE, Leslie E. **Quantum Mechanics: A Modern Development Second Edition**. [S.l.]: World Scientific Publishing Company, 2014.

BAUMGRATZ, Tillmann; CRAMER, Marcus; PLENIO, Martin B. Quantifying coherence. **Physical review letters**, APS, v. 113, n. 14, p. 140401, 2014.

BELL, John S. On the einstein podolsky rosen paradox. **Physics Physique Fizika**, APS, v. 1, n. 3, p. 195, 1964.

BENGTSSON, I; ZYCZKOWSKI, K. **Geometry of Quantum State**. [S.l.]: Cambridge University Press, 2006.

BERNSTEIN, Ethan; BERNSTEIN, Ethan. Umesh" Vazirani. Quantum complexity theory. IN PROC. In: 25TH ANNUAL ACM SYMPOSIUM ON THEORY OF COMPUTING, ACM. [S.l.: s.n.], 1993. P. 11–20.

BOIXO, Sergio; SOMMA, Rolando D. Parameter estimation with mixed-state quantum computation. **Physical Review A**, APS, v. 77, n. 5, p. 052320, 2008.

BRAUNSTEIN, Samuel L; CAVES, Carlton M. Wringing out better Bell inequalities. **Annals of Physics**, Elsevier, v. 202, n. 1, p. 22–56, 1990.

BRIEGEL, Hans J et al. Measurement-based quantum computation. **Nature Physics**, Nature Publishing Group, v. 5, n. 1, p. 19–26, 2009.

CAVALCANTI, Daniel et al. Operational interpretations of quantum discord. **Physical Review A**, APS, v. 83, n. 3, p. 032324, 2011.

CLAUSER, John F et al. Proposed experiment to test local hidden-variable theories. **Physical review letters**, APS, v. 23, n. 15, p. 880, 1969.

COSTA, Ana Cristina Sprotte. Correlações quânticas em sistemas de dois Qbits, 2012.

CURTY, M et al. Quantum correlations as basic resource for quantum key distribution. **Quantum Information Processing**, Wiley Online Library, p. 44–57, 2005.

DAKIĆ, Borivoje; VEDRAL, Vlatko; BRUKNER, Časlav. Necessary and sufficient condition for nonzero quantum discord. **Physical review letters**, APS, v. 105, n. 19, p. 190502, 2010.

DATTA, Animesh. Studies on the role of entanglement in mixed-state quantum computation. **arXiv preprint arXiv:0807.4490**, 2008.

DATTA, Animesh; FLAMMIA, Steven T; CAVES, Carlton M. Entanglement and the power of one qubit. **Physical Review A**, APS, v. 72, n. 4, p. 042316, 2005.

DATTA, Animesh; SHAJI, Anil; CAVES, Carlton M. Quantum discord and the power of one qubit. **Physical review letters**, APS, v. 100, n. 5, p. 050502, 2008.

DATTA, Animesh; VIDAL, Guifre. Role of entanglement and correlations in mixed-state quantum computation. **Physical Review A**, APS, v. 75, n. 4, p. 042310, 2007.

DE WOLF, Ronald. Quantum computing: Lecture notes. **arXiv preprint arXiv:1907.09415**, 2019.

DEUTSCH, David. Quantum theory, the Church–Turing principle and the universal quantum computer. **Proceedings of the Royal Society of London. A. Mathematical and Physical Sciences**, The Royal Society London, v. 400, n. 1818, p. 97–117, 1985.

DEUTSCH, David Elieser. Quantum computational networks. **Proceedings of the Royal Society of London. A. Mathematical and Physical Sciences**, The Royal Society London, v. 425, n. 1868, p. 73–90, 1989.

EINSTEIN, Albert; PODOLSKY, Boris; ROSEN, Nathan. Can quantum-mechanical description of physical reality be considered complete? **Physical review**, APS, v. 47, n. 10, p. 777, 1935.

EKERT, Artur K. Quantum cryptography based on Bell's theorem. **Physical review letters**, APS, v. 67, n. 6, p. 661, 1991.

FANO, Ugo. Pairs of two-level systems. **Reviews of Modern Physics**, APS, v. 55, n. 4, p. 855, 1983.

FARHI, Edward et al. Quantum computation by adiabatic evolution. **arXiv preprint quant-ph/0001106**, 2000.

FERRARO, A et al. Almost all quantum states have nonclassical correlations. **Physical Review A**, APS, v. 81, n. 5, p. 052318, 2010.

FEYNMAN, Richard P. Simulating physics with computers. **International journal of theoretical physics**, Springer, v. 21, n. 6, p. 467–488, 1982.

GISIN, Nicolas. Bell's inequality holds for all non-product states. **Physics Letters A**, North-Holland, v. 154, n. 5-6, p. 201–202, 1991.

HENDERSON, Leah; VEDRAL, Vlatko. Classical, quantum and total correlations. **Journal of physics A: mathematical and general**, IOP Publishing, v. 34, n. 35, p. 6899, 2001.

HENSEN, Bas et al. Loophole-free Bell inequality violation using electron spins separated by 1.3 kilometres. **Nature**, Nature Publishing Group, v. 526, n. 7575, p. 682–686, 2015.

HORN, Roger A; JOHNSON, Charles R. **Matrix analysis**. [S.l.]: Cambridge university press, 2012.

HORODECKI, Pawel. Separability criterion and inseparable mixed states with positive partial transposition. **Physics Letters A**, Elsevier, v. 232, n. 5, p. 333–339, 1997.

HORODECKI, Ryszard; HORODECKI, Pawel; HORODECKI, Michal. Violating Bell inequality by mixed spin-12 states: necessary and sufficient condition. **Physics Letters A**, Elsevier, v. 200, n. 5, p. 340–344, 1995.

HORODECKI, Ryszard; HORODECKI, Paweł; HORODECKI, Michał; HORODECKI, Karol. Quantum entanglement. **Reviews of modern physics**, APS, v. 81, n. 2, p. 865, 2009.

JOZSA, Richard; LINDEN, Noah. On the role of entanglement in quantum-computational speed-up. **Proceedings of the Royal Society of London. Series A: Mathematical, Physical and Engineering Sciences**, The Royal Society, v. 459, n. 2036, p. 2011–2032, 2003.

KENT, Adrian; LINDEN, Noah; MASSAR, Serge. Optimal entanglement enhancement for mixed states. **Physical review letters**, APS, v. 83, n. 13, p. 2656, 1999.

KNILL, Emanuel; LAFLAMME, Raymond. Power of one bit of quantum information. **Physical Review Letters**, APS, v. 81, n. 25, p. 5672, 1998.

LANYON, BP et al. Experimental quantum computing without entanglement. **Physical review letters**, APS, v. 101, n. 20, p. 200501, 2008.

MAZIERO, J; CELERI, LC; SERRA, RM. Symmetry aspects of quantum discord. **arXiv preprint arXiv:1004.2082**, 2010.

MODI, Kavan; BRODUTCH, Aharon, et al. The classical-quantum boundary for correlations: discord and related measures. **Reviews of Modern Physics**, APS, v. 84, n. 4, p. 1655, 2012.

MODI, Kavan; CABLE, Hugo, et al. Quantum correlations in mixed-state metrology. **Physical Review X**, APS, v. 1, n. 2, p. 021022, 2011.

NAKANO, Takafumi; PIANI, Marco; ADESSO, Gerardo. Negativity of quantumness and its interpretations. **Physical Review A**, APS, v. 88, n. 1, p. 012117, 2013.

NIELSEN, Michael A; CHUANG, Isaac L. **Quantum computation and quantum information**. [S.l.]: Cambridge University Press, Cambridge, 2000.

OLLIVIER, Harold; ZUREK, Wojciech H. Quantum discord: a measure of the quantumness of correlations. **Physical review letters**, APS, v. 88, n. 1, p. 017901, 2001.

OZOLS, Maris. **How to generate a random unitary matrix**. [S.l.]: Technical Report, 2009.

PARKER, S; PLENIO, Martin B. Efficient factorization with a single pure qubit and log N mixed qubits. **Physical review letters**, APS, v. 85, n. 14, p. 3049, 2000.

PASSANTE, Gina. On Experimental Deterministic Quantum Computation with One Quantum Bit (DQC1). University of Waterloo, 2012.

PASSANTE, G et al. Experimental detection of nonclassical correlations in mixed-state quantum computation. **Physical Review A**, APS, v. 84, n. 4, p. 044302, 2011.

PERES, Asher. Separability criterion for density matrices. **Physical Review Letters**, APS, v. 77, n. 8, p. 1413, 1996.

POULIN, David et al. Exponential speedup with a single bit of quantum information: Measuring the average fidelity decay. **Physical review letters**, APS, v. 92, n. 17, p. 177906, 2004.

RAU, ARP et al. Calculation of quantum discord for qubit-qudit or N qubits. **arXiv preprint arXiv:1106.4488**, 2011.

RAUSSENDORF, Robert; BROWNE, Daniel E; BRIEGEL, Hans J. Measurement-based quantum computation on cluster states. **Physical review A**, APS, v. 68, n. 2, p. 022312, 2003.

ROSSATTO, Daniel Zini et al. Correlações quânticas e transição quântico-clássica em cavidades ópticas. Universidade Federal de São Carlos, 2014.

SANTOS, Márcio Macedo et al. Correlações quânticas e o modelo DQC1. Universidade Federal de Uberlândia, 2015.

SCHRÖDINGER, Erwin. Discussion of probability relations between separated systems. In: CAMBRIDGE UNIVERSITY PRESS, 4. MATHEMATICAL Proceedings of the Cambridge Philosophical Society. [S.l.: s.n.], 1935. P. 555–563.

SHANNON, Claude E. A mathematical theory of communication. **Bell system technical journal**, Wiley Online Library, v. 27, n. 3, p. 379–423, 1948.

SHAO, Lian-He et al. Fidelity and trace-norm distances for quantifying coherence. **Physical Review A**, APS, v. 91, n. 4, p. 042120, 2015.

SHOR, Peter W. Algorithms for quantum computation: discrete logarithms and factoring. In: IEEE. PROCEEDINGS 35th annual symposium on foundations of computer science. [S.l.: s.n.], 1994. P. 124–134.

SHOR, Peter W; JORDAN, Stephen P. Estimating Jones polynomials is a complete problem for one clean qubit. **arXiv preprint arXiv:0707.2831**, 2007.

SIMON, Daniel R. On the power of quantum computation. **SIAM journal on computing**, SIAM, v. 26, n. 5, p. 1474–1483, 1997.

SIMON, Rajiah. Peres-Horodecki separability criterion for continuous variable systems. **Physical Review Letters**, APS, v. 84, n. 12, p. 2726, 2000.

TUFARELLI, Tommaso et al. Quantum resources for hybrid communication via qubit-oscillator states. **Physical Review A**, APS, v. 86, n. 5, p. 052326, 2012.

VAIDMAN, Lev. Teleportation of quantum states. **Physical Review A**, APS, v. 49, n. 2, p. 1473, 1994.

VAN DAM, Wim; MOSCA, Michele; VAZIRANI, Umesh. How powerful is adiabatic quantum computation? In: IEEE. PROCEEDINGS 42nd IEEE Symposium on Foundations of Computer Science. [S.l.: s.n.], 2001. P. 279–287.

VEDRAL, Vlatko et al. Quantifying entanglement. **Physical Review Letters**, APS, v. 78, n. 12, p. 2275, 1997.

VIDAL, Guifré; WERNER, Reinhard F. Computable measure of entanglement. **Physical Review A**, APS, v. 65, n. 3, p. 032314, 2002.

WERNER, Reinhard F. Quantum states with Einstein-Podolsky-Rosen correlations admitting a hidden-variable model. **Physical Review A**, APS, v. 40, n. 8, p. 4277, 1989.

YU, Xiao-Dong et al. Alternative framework for quantifying coherence. **Physical Review A**, APS, v. 94, n. 6, p. 060302, 2016.

ZYCZKOWSKI, Karol; KUS, Marek. Random unitary matrices. **Journal of Physics A: Mathematical and General**, IOP Publishing, v. 27, n. 12, p. 4235, 1994.

ŻYCZKOWSKI, Karol et al. Generating random density matrices. **Journal of Mathematical Physics**, American Institute of Physics, v. 52, n. 6, p. 062201, 2011.

APPENDIX A – CUMULATIVE η

A program was built in MATLAB that returns us a purified auxiliary qubit, with purity $P(\rho) > 0.5$, which is the initial purity of the auxiliary qubit, whose initial state is $\frac{I}{2}$. This program draws a random η between a defined value among 13 predefined values (section 4.2.1) and 1. After this draw, we run the filter optimization program until obtaining a defined cumulative value (one of the 13 possible values). So, at the end we have a filter parameter value that generates a more purified auxiliary qubit. In summary, the idea of this program is that the first η used in the purification of the auxiliary qubit is a number between a value define and 1, the next between this previous value and 1 (decreasing the distance), until reaching the cumulative chosen value. With this final cumulative η we analyze what purity the qubit auxilir reached.